Ecological Modelling 427 (2020) 109003

Contents lists available at ScienceDirect

Ecological Modelling

journal homepage: www.elsevier.com/locate/ecolmodel

Environmental and behavioral controls on juvenile Chinook salmon migration pathways in the Columbia River estuary

Katherine J. Morrice (Conceptualization; Formal Analysis; Investigation; Methodology; Visualization; Writing – original draft; Writing – review & editing)[a,*], António M. Baptista (Supervision; Conceptualization; Writing – review & editing)[a], Brian J. Burke (Conceptualization; Writing – review & editing)[b]

[a] Oregon Health & Science University, 3181 SW Sam Jackson Park Rd., Portland, OR 97239, United States
[b] Fish Ecology Division, National Marine Fisheries Science Center, National Oceanic and Atmospheric Administration, 2725 Montlake Boulevard East, Seattle, WA 98112, United States

ARTICLE INFO

Keywords:
Juvenile Chinook salmon
Columbia River estuary
Individual-based model
Estuarine migration
Estuarine behavior

ABSTRACT

Juvenile Chinook salmon population dynamics in the Columbia River estuary are influenced by physical processes, hatchery practices, and behavioral decision-making. To better understand how environmental forcing and swimming behavior influence estuarine migration and travel times, we developed an individual-based model (IBM) that uses 3-D outputs from a hydrodynamic model to simulate Lagrangian transport as well as swimming and bioenergetics sub-models to simulate active swimming and growth. Simulations were run in 2010 during the migration seasons for yearling and subyearling Chinook salmon. For both life history types, alternative behaviors were simulated, from random walks to behaviors that optimized efficient system migration for yearling Chinook salmon and growth for subyearling Chinook salmon. Simulation results compared well against observed data on travel times and common migration pathways; the simulated travel times for both yearling and subyearling Chinook salmon were within several hours of the observed travel times. In general, residence times and pathways were largely driven by river discharge and the phase of the tide. During periods of greater river discharge, simulated estuarine residence times were reduced and variability across individuals was minimal. The timing of estuarine exit was closely tied to the phase of the tide, with most simulated individuals exiting the system during the ebb phase. While travel times were largely driven by flow velocities, swimming behavior was likewise important. Simulated yearling Chinook salmon behaviors that optimized movement with surrounding flows resulted in reduced estuarine residence times when compared to passive and random walk behaviors. Similarly, simulated subyearling Chinook salmon behaviors that optimized growth directed individuals to shallow peripheral habitats, resulting in longer residence times and higher growth rates. Even if potentially important factors such as predator avoidance were not included, this IBM provides an informative tool to model migration pathways, growth, and residence times of juvenile salmon in an estuarine environment and could be used to inform management decisions by evaluating various scenarios.

1. Introduction

The Columbia River basin serves as important habitat for anadromous fish in the Pacific Northwest. The river and its surrounding tributaries have historically supported large runs of several species of salmonids; however, habitat loss, hydropower development, navigation improvements, and overfishing in the past century, have all contributed to their decline (Bottom et al., 2005). Furthermore, an increasing shift of hatcheries towards production-oriented practices has reduced salmonid diversity and residency in the Columbia River estuary (Bottom et al., 2005). Due to these ongoing stressors, thirteen stocks are now listed under the Endangered Species Act (ESA) as threatened or endangered (Myers et al., 1998). As a result of these listings, there is a pressing need for an improved understanding of salmonid survival and migratory behaviors to inform recovery efforts and habitat restoration.

The importance of estuarine habitat has been of particular interest, especially with regards to how the Federal Columbia River Hydropower System (FCRPS) has altered juvenile rearing habitats and overall

* Corresponding author.
E-mail address: morricek@ohsu.edu (K.J. Morrice).

https://doi.org/10.1016/j.ecolmodel.2020.109003
Received 3 October 2019; Received in revised form 23 December 2019; Accepted 20 February 2020
Available online 30 April 2020

production. Estuaries are important rearing habitats for salmonids that provide multiple services, including food resources, shelter from predators, and a transitional habitat to physiologically adapt to increasing salinities (Bottom et al., 2005; Simenstad et al., 1982; Thorpe, 1994). However, estuaries can also be challenging environments due to tides, strong and dynamic salinity gradients, and increasing interactions with predators. Juvenile Pacific salmon use estuaries to varying degrees (Bottom et al., 2005; Healey, 1982; Simenstad et al., 1982), and populations have adapted to using freshwater and estuarine habitats in different capacities.

Diverse migration patterns across life-history types result in a wide range of estuarine residence times (Weitkamp et al., 2014). For yearling salmonids, estuarine residence times are on the order of days to weeks, while estuarine residence times for subyearling salmonids often last weeks to months (Healey, 1982; Simenstad et al., 1982). Yearling salmonids migrate to the ocean after rearing in freshwater for a year or more (i.e., coho, sockeye, steelhead, and stream-type Chinook) and typically travel quickly through the estuary, using it as a migration corridor. They are often assumed to minimally interact with estuarine habitat outside of the main channels; however, recent work by McNatt and Hinton (2017) observed yearling Chinook salmon in wetland habitats, thereby challenging this assumption. Subyearling salmonids (i.e., ocean-type Chinook and chum) spend less time rearing in freshwater and instead migrate earlier and spend longer periods in estuaries (Healey, 1982; Quinn, 2005; Weitkamp et al., 2014). Whereas yearling salmonids do not spend much time in shallow habitats, smaller subyearling salmonids frequently occupy shallow nearshore wetland habitats (McCabe et al., 1986; Simenstad et al., 1982).

Smolts generally migrate between May and July, responding to environmental cues such as the spring freshet. Juvenile salmon that have shorter estuarine residence migrate earlier in the season, while those with longer estuarine residence migrate mid-summer (Healey, 1982; Roegner et al., 2012; Weitkamp et al., 2012). As juveniles migrate from freshwater to marine environments, they experience different habitats and environmental conditions, and this variation impacts the timing of their migration and size at ocean entry. Smolt migration rate and survival are affected by a number of factors, including predation, physiology, river flows, and ocean conditions. Although there have been concerted efforts to study smolt survival along the hydropower system upstream of Bonneville Dam, less is known about how survival changes downstream of Bonneville Dam as smolts continue their migration through the estuary.

Field-based campaigns and modeling efforts have advanced our understanding of juvenile salmonid habitat preference, survival, and migration in the estuary. However, these studies are often of limited temporal or spatial scope and may underrepresent distributions of juvenile salmon, particularly in shallow nearshore environments. Passive integrated transponder (PIT) tag (Ledgerwood et al., 2004; Prentice et al., 1990) and the Juvenile Salmon Acoustic Telemetry System (JSATS) tag (McMichael et al., 2010) data have been especially useful for tracking survival and migration rates; however, such data are typically collected at a select few locations and thus lack comprehensive information about the entire migratory pathway.

Modeling approaches have also been used to quantify optimal habitat for juvenile Chinook salmon and how that changes based on river discharge (Kukulka and Jay, 2003a, b), tides, and seasons. Salmon habitat opportunity (Bottom et al., 2005; Burla, 2009), an area-based metric, and salmon habitat (Rostaminia, 2017), a volume-based metric have both been used to compute the amount of optimal salmon habitat available in specific hydrogeomorphic reaches of the estuary. Although these methods are informative to understanding how different reaches of the estuary function as habitat over time, these Eulerian-based approaches do not account for how juvenile salmon interact with and respond to changing environmental conditions along a migration route. Furthermore, these methods have relied solely on physical variables (e.g., temperature, salinity, flow velocities, and water depths) and do not account for biological habitat components.

A more in-depth investigation of how the estuary supports stocks of juvenile salmon is needed and requires a modeling technique that tracks estuarine residence and migration pathways of individual salmon. This can be addressed with an individual-based model (IBM) that simulates juvenile salmon migration in the estuary, providing a means to characterize how system variability and behavioral decisions affect estuarine migration pathways. IBMs are effective tools for tracking the spatial and temporal distributions of organisms and their response to biotic and abiotic environmental conditions. When coupled with bioenergetics models, IBMs can offer insight into the response of individual growth to environmental variability (Fiechter et al., 2015a; Hinckley et al., 1996).

IBMs vary in their level of sophistication. Some IBMs simulate extensive life-history processes and consider foraging, growth, mortality, and reproduction, while others are simpler and employ rule-based methods to approximate movement patterns and habitat use (Giske et al., 1998; Tyler and Rose, 1994). IBMs are frequently used to describe distributions of marine fish populations (Miller, 2007) and have been adapted to simulate salmon migration pathways in the ocean (Byron and Burke, 2014). In addition, IBMs have been applied to the upstream reaches of the Columbia River to investigate juvenile salmon passage through the hydropower system (Goodwin et al., 2006), as well as to the Columbia River plume (Brosnan, 2014) and coastal ocean off Oregon and Washington (Burke et al., 2014, 2016). Although IBMs have been used in upstream reaches of the Columbia River and off the mouth of the estuary, there have been few attempts to simulate juvenile Chinook salmon in the estuary.

The objectives of this work were to investigate potential estuarine migration pathways of yearling and subyearling Chinook salmon in the Columbia River estuary using different swimming behaviors and to explore how environmental conditions and behavioral decisions influence migration pathways, travel times, and growth rates. To address these objectives, an IBM coupled with a bioenergetics model was used to simulate movement due to advection and active swimming and growth based on the local environment. Results from model simulations were then validated against observations to assess model performance. Chinook salmon were the focus of this study as they are the most estuarine-dependent salmonid species in the Columbia River (Healey, 1982). In addition, there are multiple species of Chinook salmon listed as endangered or threatened under the ESA, and multiple life-history strategies for each species, allowing for an intra-specific behavioral comparison.

2. Methods

2.1. Overview

An IBM was used to simulate juvenile Chinook salmon migration in the Columbia River estuary from Bonneville Dam to the estuary mouth (Fig. 1). The virtual environment wherein fish movement and growth were modeled utilized outputs from a hydrodynamic model. Data collected at Bonneville Dam and various locations in the estuary informed model design (e.g., simulation timing, starting fish lengths, and length-weight relationships). In addition, acoustic telemetry data from multiple regions of the Columbia River estuary were used to assess the performance of the IBM. Wetland habitat quality, adapted from the Lower Columbia Estuary Partnership (LCEP) land cover dataset (Sanborn Map Company, 2011) was used as a proxy for feeding success in the bioenergetics model. Fish were modeled using different swimming behaviors, and results from these simulations were then analyzed to describe travel times, migration pathways, and growth. In addition, the effects of river and tidal forcing were considered.

The year of focus for this work was 2010. This year was selected because there was a large number of detections of juvenile Chinook salmon in the Columbia River estuary pair-trawl experiment in 2010

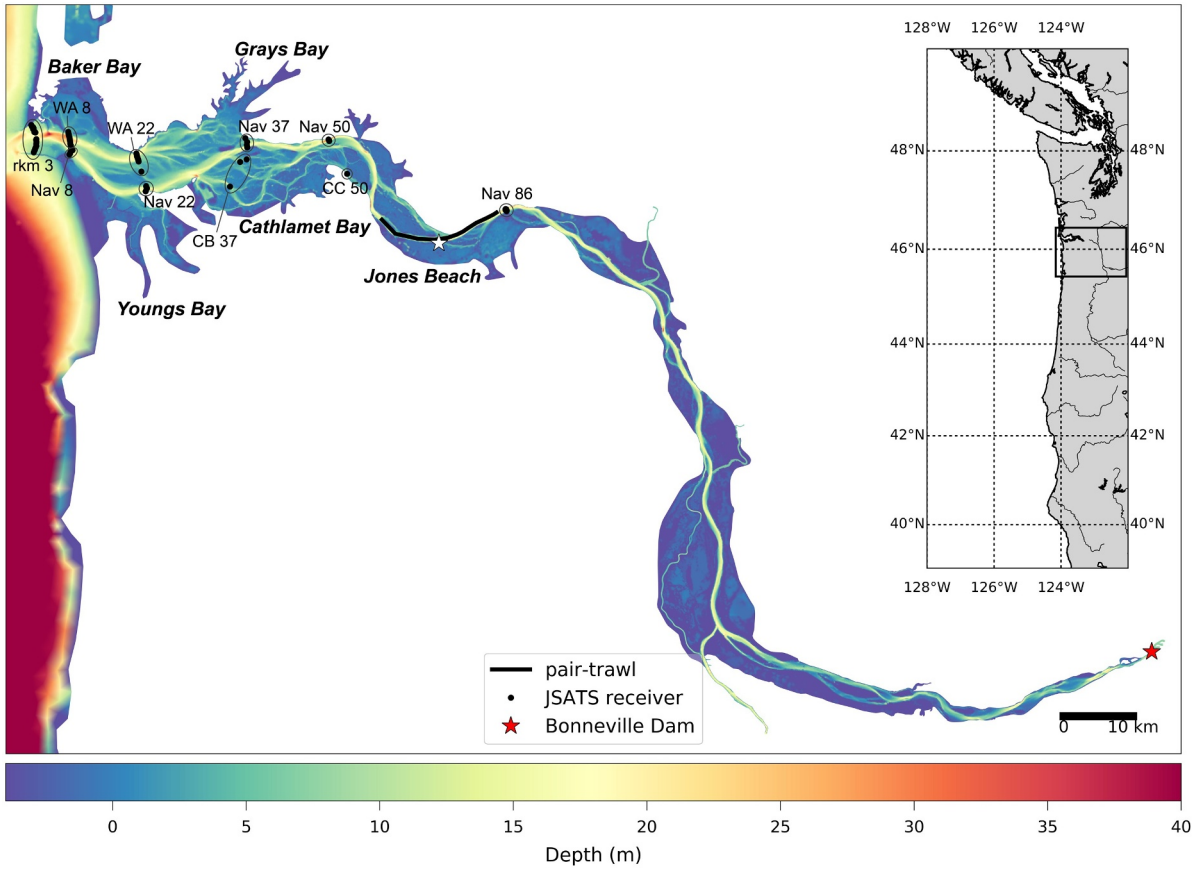

Fig. 1. Map of the simulated virtual environment. The inset represents the entire region simulated in the hydrodynamic model, with the outlined region representing the Columbia River estuary. The bathymetry of the estuary is represented as well as locations of specific interest, including Bonneville Dam, where fish were initialized, the region sampled by the pair-trawl near Jones Beach, the lateral bays, and the locations of JSATS nodes that constitute cross-channel arrays in the lower estuary. Array locations with the Nav prefix are located in the navigation channel, while those with different prefixes are located in peripheral or secondary channels (e.g., CC = Clifton Channel, CB = Cathlamet Bay, WA = Washington shoreline). (For interpretation of the references to color in this figure legend, the reader is referred to the web version of this article.)

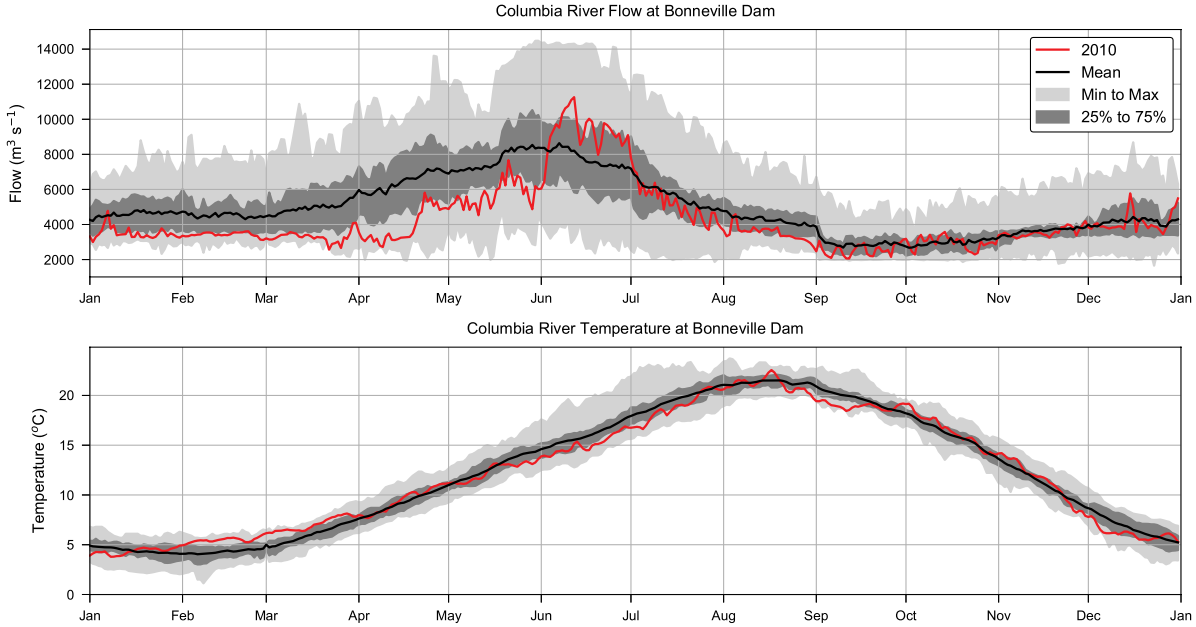

Fig. 2. Daily Columbia River flows ($m^3\ s^{-1}$) (*top*) and daily temperatures (°C) (*bottom*) at Bonneville Dam in 2010 (red), in addition to mean, 25–75% percentiles, and minimum and maximum values from 1999–2016. (For interpretation of the references to color in this figure legend, the reader is referred to the web version of this article.)

and because there were abundant JSATS data in the lower estuary. Flows in 2010 started below average but rose substantially by early June (Fig. 2), with above-average flows for most of June. Major flows associated with the spring freshet were slightly delayed when compared to historical mean flows. Temperatures recorded at Bonneville Dam were relatively low at Bonneville during the spring season; however, by late summer, temperatures exceeded 20 °C.

The following sections describe the juvenile salmon data used to inform simulation design and to assess model performance, the hydrodynamic model used to generate the virtual environment, the framework and details of the IBM, and how model results were analyzed.

2.2. Juvenile salmon data

Every year, data are collected on the timing and survival of juvenile Chinook salmon as they pass through the hydropower system and Columbia River estuary. Passive integrated transponder (PIT) tags are implanted in a portion of juvenile salmonids to track migration timing and survival. As individual fish pass juvenile monitoring stations located at the dams, their tag code and the date and time of detection are recorded. The PIT tag data are then uploaded to the Columbia Basin PIT Tag Information System (PTAGIS, available at http://www.ptagis.org). The JSATS, developed by the Pacific Northwest National Laboratory and NOAA Fisheries for the U.S. Army Corps of Engineers, also monitors juvenile salmonid survival and travel times in the Columbia River, lower estuary, and plume. The JSATS tags last for approximately 30 days, whereas the PIT tags last for years, remaining functional throughout the fish's lifespan. The detection range of 300 m in the JSATS system (McMichael et al., 2010) is greater than the detection range for PIT tags which typically must be within 10–100 cm of an antenna to be detected.

Downstream of Bonneville Dam, the last hydroelectric dam in the hydropower system, a pair-trawl is deployed from late March through early August in the lower estuary between Eagle Cliff (rkm 83) and Puget Island (rkm 61) (Fig. 1). The pair-trawl study targets migrating juvenile Chinook salmon and steelhead, and data collected from this long-term study inform survival estimates of migrating juvenile salmonids and comparisons between in-river migrants and barged fish that are transported and released below Bonneville Dam (Ledgerwood et al., 2004). In 2010, there were more than 100,000 spring/summer (i.e. yearling) Chinook salmon and 28,698 fall (i.e. subyearling) Chinook salmon that were PIT-tagged and detected at Bonneville Dam. Of the Chinook salmon detected at Bonneville Dam, 3632 spring/summer and 461 fall Chinook salmon were detected in the pair-trawl, representing detection rates of 3.6% and 1.6%.

As part of the 2010 JSATS study (Harnish et al., 2012), acoustic telemetry receivers were deployed in the navigation channel and off-channel areas from the estuary mouth to rkm 86 in depths of at least 4 m (Fig. 1). Data were collected from these cross-channel arrays from late April to August and later analyzed to describe common migration pathways, travel times, and survival of migrating juvenile Chinook salmon and steelhead in the lower estuary. There were 3880 yearling Chinook salmon and 4449 subyearling Chinook salmon that were tagged and released in the 2010 JSATS study (Harnish et al., 2012). Subyearling Chinook salmon included in the study were slightly larger than the general population, as only individuals greater than 95 mm in fork length were targeted (Harnish et al., 2012).

2.3. Hydrodynamic model

Hindcast simulations using the unstructured grid, finite element model SELFE (Zhang and Baptista, 2008) served as the virtual environment for the IBM. This 3-D hydrodynamic model has been benchmarked for the Columbia River estuary (Kärnä and Baptista, 2016a; Kärnä et al., 2015), and data collected by numerous instruments throughout the estuary (Baptista et al., 2015) have been used to evaluate model skill. SELFE solves a set of nonlinear, baroclinic, shallow-water equations. The unstructured grid consists of triangular elements in the horizontal that extend in the vertical dimension to form 3-D prisms. The vertical grid in shallow regions is based on a hybrid terrain-following and free-surface adapted S grid (Song and Haidvogel, 1994). Outside of the estuary, the surface grid transitions to an equipotential z grid starting at the 100 m isobath.

The model is driven by multiple forcings taken from larger-scale models. Atmospheric forcing is from the NOAA/NCEP North American Mesoscale Forecast System and includes wind velocities, shortwave and longwave radiation, air temperature, and pressure (Rogers et al., 2009). The tides come from a regional inverse model (Myers and Baptista, 2001) and are applied along the ocean boundary. Temperature, salinity, and water elevations from the global Navy Coastal Ocean Model (NCOM) (Barron et al., 2006) are also imposed along the ocean boundary. Starting near the ocean boundary and extending approximately 50 km into the domain, temperature and salinity values computed by SELFE are nudged to NCOM values to prevent values from drifting significantly from NCOM. River discharge, elevations, and water temperatures from USGS are used as riverine forcing from the Columbia and Willamette rivers, as well as smaller tributaries, the Lewis and Cowlitz rivers.

The horizontal mesh extends from northern California to Vancouver Island (39°N to 50°N) and from the Columbia River near Bonneville Dam (river kilometer 234) to 300 km offshore (Fig. 1). There are 89,819 nodes, and 173,800 elements, and domain resolution is highest in the estuary, where resolution is typically between 100–200 m. The resolution becomes coarser past the estuary in the plume (200–1000 m) and is less resolved in the ocean (>1 km). The time step used in the circulation model is 36 s, and outputs are stored every fifteen minutes.

2.4. Individual-based model

Our IBM is described using the overview, design concepts, and details (ODD) protocol for IBMs outlined in Grimm et al. (2006). The purpose of the model as well as the structure and low-level entities are first described. This is followed by the design concepts that provide the framework for the IBM and the details that describe how the model is initialized, what inputs are used, and descriptions of the sub-models. A diagram of the model is shown in Fig. 3.

2.4.1. Overview

2.4.1.1. Purpose. The purpose of the IBM is to investigate potential migration pathways and travel times of juvenile Chinook salmon in the Columbia River estuary. This was accomplished by simulating multiple swimming behaviors of varying complexity in addition to passive drift. Although there are long-term studies describing travel times to various reaches in the estuary, not enough is known about how environmental processes and swimming behavior influence estuarine residence and growth of juvenile Chinook salmon. The high spatiotemporal resolution of the IBM provides an effective means for evaluating how environmental processes (e.g. river discharge and tides) and behavioral decisions affect migration pathways and residence times. Results from model simulations are compared against observational data on travel times and preferred estuarine migration pathways to evaluate the model's performance.

2.4.1.2. State variables and scales. The IBM is made up of multiple low-level entities that include environmental state variables and individual-based variables. The environmental state variables from the hydrodynamic model included water temperatures, 3-D flow velocities, and water depths. In addition, a habitat index that relates to the bioenergetics model was used. The temporal resolution of the environmental variables was fifteen minutes, with the exception of the habitat index that was constant over time. In some simulations, the estuary's hydrogeomorphic reach was considered, as well as geographic

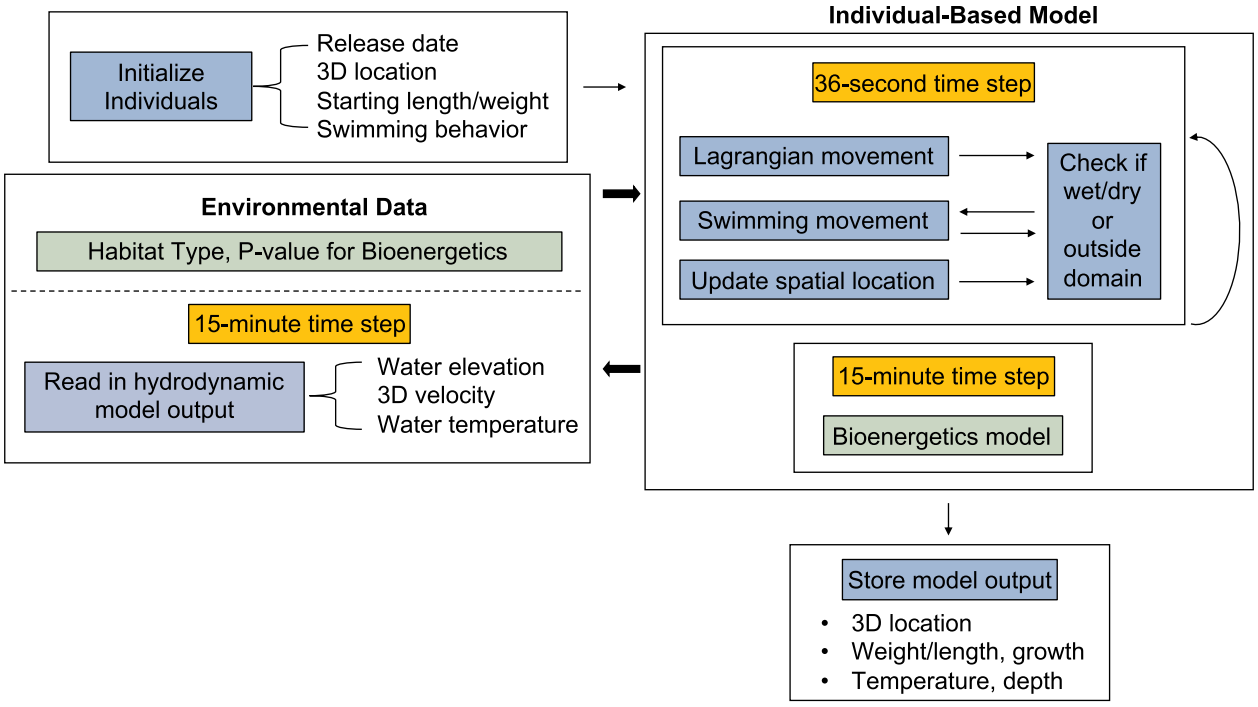

Fig. 3. Conceptual diagram of the IBM. Individuals are initialized and environmental data are read in, including global variables relating to the bioenergetics model and output from a hydrodynamic model with a 15-min time step. At every 15-min time step, individual movement is simulated using a 36-s time step and loops through until the end of that period. Following that, growth is computed using the bioenergetics model, and output is stored for that time step before proceeding to the next time step.

targets within these reaches that correspond with the downstream extent of that reach.

The variables describing individual fish included their initial location and size (defined by fork length and weight). Growth was simulated using a bioenergetics model, where growth rates were dependent on water temperatures, fish size, the proportion of maximum consumption (*P*-value), and prey energy density. Fish were initialized near Bonneville Dam and assigned a 3-D location and date of estuarine entry.

2.4.1.3. Process overview and scheduling. Simulations were conducted from March 13 to August 4 for yearling Chinook salmon and from April 25 to November 3 for subyearling Chinook salmon and correspond with statistics on run timing at Bonneville Dam. The last dates of initialization were July 5 for yearlings and September 4 for subyearlings to ensure adequate time for individuals to exit the estuary. These dates and the number of individuals simulated over time were based on normal distributions of run timing data (see section 2.4.3.1.). Each model run commenced at 00:15 am (PST) on the first date of initialization. Environmental state variables were read in every fifteen minutes, and values at finer temporal resolutions corresponding with the IBM time step were linearly interpolated.

Movement due to advection, followed by movement due to active swimming, was calculated every 36 s, and the new location was stored every fifteen minutes. At the end of each fifteen-minute time step, individual growth was calculated using the bioenergetics model which factors in the temperature of the currently occupied position and the *P*-value assigned to the occupied element. Mortality, predation, and density-dependent interactions were not considered in the model. If all individuals exited the estuary prior to the end date of the simulation, the simulation ended early.

2.4.2. Design concepts

2.4.2.1. Basic principles. The IBM describes the migration of yearling and subyearling Chinook salmon through a heterogenous environment, where individuals go from narrow upstream reaches of the river to an increasingly tidally-influenced environment. As they move through this system, they can adopt a number of strategies that ultimately shape their migration pathways. Yearling Chinook salmon that are known to use the system as a migration corridor are more likely to occupy the main navigation channels, whereas subyearling Chinook salmon spend greater time in the estuary, particularly in shallow-water habitats. There are therefore two different strategies to explore when it comes to simulating swimming behavior, one that optimizes efficient migration through the system, and one that optimizes growth in the estuary. The behavioral rules implemented for yearling Chinook salmon include directed migration optimizing timely estuarine exit, whereas the rules for subyearling Chinook salmon include reactive or directed movement to regions with high growth-rate potential.

Swim speeds are size-dependent (Ware, 1978), and it is recognized that larger salmon migrate more quickly through estuaries (Dawley et al., 1986; Healey, 1982). Therefore, it is necessary to track changes in fork length over time, as that affects travel times. The bioenergetics model computes growth over time based on the environmental conditions experienced, and as fish increase in length throughout the simulation, so too does their swim speed.

The bioenergetics model used a constant prey energy density and a *P*-value, the proportion of maximum daily consumption, that depended on habitat type. To factor differences in habitat quality into the bioenergetics model, *P*-values were based on the presence or proximity to wetland habitat. Elements classified as wetland habitat as well as the immediately neighboring elements had a *P*-value of 0.9, whereas outside of these regions, the *P*-value was 0.5. This allowed for a benefit to be factored in that considered preferred rearing habitats and relative feeding habits in these regions. This approach of classifying *P*-values based on habitat was similarly implemented in Brosnan (2014).

2.4.2.2. Sensing and prediction. For simulated yearling Chinook salmon, under the more complex behavioral rules (e.g. negative rheotaxis and biased correlated random walk), individuals factored environmental states into their decisions. Under the negative rheotaxis behavior, fish

oriented their movement to align with the direction of prevailing flows, and could therefore sense their immediate flow environment. Under the biased correlated random walk behavior, fish movement was correlated with the movement calculated from the previous time step, and thus considered movement both due to advection and active swimming. In addition, the bias term directed fish to move downstream by orienting fish to move towards the downstream extent of each hydrogeomorphic reach. Thus, individuals simulated under this behavior had a predictive sense of what direction to swim in, based on the assumption that individuals optimize movement towards the ocean.

For simulated subyearling Chinook salmon, under the more complex behavioral rules (e.g. kinesis and restricted-area search), individuals sensed and/or predicted the growth rate potential of their environment. Individuals simulated using the kinesis behavior considered their immediate environment, and their swim speed and direction were based on the computed rate of consumption of the current position against an optimal rate of consumption. For individuals simulated using the restricted-area search behavior, they sensed their surrounding environment, and evaluated the growth rate potential of the immediately neighboring elements, where the average distance to neighbors was approximately 140 m. While the restricted-area search behavior accounted for both gains (i.e. consumption) and losses (e.g., respiration, egestion, and excretion) the kinesis behavior only considered gains.

2.4.2.3. Stochasticity. Simulations across the different behaviors were all started using the same random number seed. The random seed was used to initialize the starting location, initial lengths and weights, and date of entry for each of the different behaviors that were simulated. This means that all simulations started with the same initial conditions, but they varied in the swimming behavior that was applied. Noise was also added to the model in the form of random noise that was added to individual swimming behavior.

2.4.2.4. Observation. After every fifteen-minute time step, the location and the length and weight of each fish were recorded. In addition, environmental variables were stored, including the temperature, water depth, and occupied element.

2.4.3. Details

2.4.3.1. Initialization. Individuals were initiated in the upstream region of the model domain near Bonneville Dam at 45°38′06”N, 121°57′41”W (Fig. 1) using a normal distribution centered at this location with a standard deviation of 20 m in the horizontal. Vertical positions within the water column were initialized using a uniform distribution between 0 and 2 m below the surface. Initial fork lengths were based on daily fish condition fork length data collected at Bonneville Dam by the Fish Passage Center Smolt Monitoring Program. The fork length data for subyearling Chinook salmon showed an increasing trend over time. To reduce the bias of these longer fork lengths when creating the distribution of subyearling Chinook salmon starting lengths, only fork length data through the end of August were considered. The starting lengths were drawn from normal distributions for yearling Chinook salmon (μ = 142.5 mm, SD = 18.7 mm) and subyearling Chinook salmon (μ = 95.6 mm, SD = 13.3 mm). A truncated normal distribution with bounds at 61 mm and 140 mm was used for the subyearling Chinook salmon to prevent lengths at the tails of the distribution. This lower threshold also marks the difference between fingerlings and smaller emergent and resident frys.

Simulation timing was based on the smolt index at Bonneville Dam from the Fish Passage Center (Fig. 4). The smolt index is based on PIT-tag detections at juvenile monitoring locations and factors in the flow magnitude to estimate the number of fish passing per day, as not all fish are detected at the monitoring locations. Passage dates for subyearling Chinook salmon prior to June were excluded when creating the run timing distribution as these detections are associated with juveniles from the previous year that were held over by hatcheries to be released as yearlings. In Fig. 4, these larger individuals with earlier run timing are represented in the first two peaks.

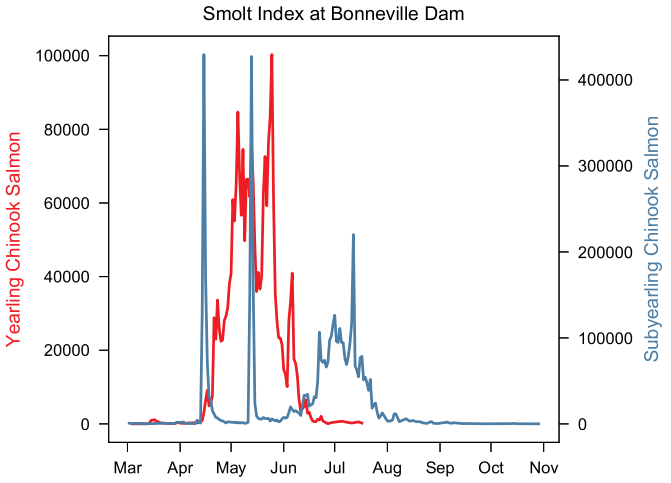

Fig. 4. Smolt index (fish day^{-1}) for yearling Chinook salmon and subyearling Chinook salmon at Bonneville Dam in 2010. (For interpretation of the references to color in this figure legend, the reader is referred to the web version of this article.)

Although it is recognized that the timing of detections for yearling and subyearling Chinook salmon do not follow normal distributions, this distribution was used to initialize times of simulated passage at Bonneville Dam in the IBM. Using the mean and standard deviation of run timing, normal distributions were generated for the yearling Chinook salmon simulation dates (μ = 133.5, SD = 13 days) and subyearling Chinook salmon simulation dates (μ = 185.5, SD = 15 days) as indicated in Table 1. These distributions corresponded with initialization dates between March 13–July 5 centered on May 13 for yearling Chinook salmon and April 25–September 4 centered on July 4 for subyearling Chinook salmon. While individuals may be detected at Bonneville outside of these date ranges, these periods pertain to the period when most individuals migrate. The times of initialization were rounded to the nearest quarter hour to correspond with the fifteen-minute time step of the hydrodynamic model output.

2.4.3.2. Input. Environmental variables (e.g., water temperatures, velocities, water depths) from the hydrodynamic model were used as model inputs. Wetland habitat data from the 2010 High Resolution Land Cover Data from LCEP was used to generate *P*-values used in the bioenergetics model, representing a proxy of habitat quality. This GIS dataset was first described in Simenstad et al. (2011) where it was applied to a particular hydrogeomorphic reach. The data include 26 different land cover classes, including tidal and non-tidal classes of coniferous, deciduous, shrub-scrub and herbaceous habitat as well as classes more representative of substrates or anthropogenic uses (e.g., agricultural, impervious surface, and developed). Juvenile salmon rely on food exported from emergent marsh habitat (Bottom et al., 2005), and macroinvertebrates associated with such habitats serve as a significant dietary source (Bottom et al., 2008). All wetland classes, with the exception of upland habitats were merged into one wetland class, and these data were then interpolated to the element centers.

2.4.3.3. Lagrangian transport sub-model. A Lagrangian method was used to simulate fish movement due to advection. The position at each time step was calculated from the previous time step according to:

$$x_{t+1} = x_t + u\delta t \quad (1)$$

$$y_{t+1} = y_t + v\delta t \quad (2)$$

$$z_{t+1} = z_t + w\delta t \quad (3)$$

Table. 1
Run timing distributions for yearling and subyearling Chinook salmon, as well as the dates the runs commenced and ended and the starting lengths.

Life-history type	Run timing	Start date	End date	Starting length
Yearling	133.5 ± 13 days	March 13	August 4	142.5 ± 18.7 mm
Subyearling	185.5 ± 15 days	April 25	November 3	95.6 ± 13.3 mm

Velocities due to advection (*u, v, w*) were computed from spatial and temporal interpolation of the flow fields, and the fish's location was updated using a Runge-Kutta fourth-order time integration method. Similar to the time step used in the hydrodynamic model, a 36 s time step was used for interpolation. This time step was preferred over the 15 min time step of the hydrodynamic model output because it improved the particle tracking skill. In addition, it reduced the frequency at which fish horizontally exited the domain or moved to dry elements, which was a common occurrence, especially in narrower reaches of the river. If fish moved to a dry element or outside of the grid due to advection, the intersection between the individual's pathway and the intersected element edge was computed, and the tangential velocity was calculated to adjust the trajectory such that the individual maintained its position within the model domain.

2.4.3.4. Swimming behavior sub-model. Swimming behavior was simulated using different movement models that varied based on assumptions about how juvenile Chinook salmon use estuarine habitat. It was assumed that yearling Chinook salmon behaviors optimize efficient migration through the system, while subyearling Chinook salmon behaviors are more driven by the search for habitat where growth is optimized. The movement models varied in complexity from simple random walks to more sophisticated behaviors that depended on local environmental conditions. While predation is of concern in the system, field data were not available at a high enough spatial and temporal resolution to inform the model. In addition, not enough is known about juvenile salmon predator avoidance swimming behaviors in the estuary.

For both yearling and subyearling Chinook salmon, passive and random walk behaviors were simulated. Under the passive behavior, individual movement was driven by advection only and no active swimming was included. The simplest swimming behavior for both life history types was an uncorrelated and unbiased random walk, where there was no behavioral response to external stimuli and the direction of movement was random (Codling et al., 2008; Willis, 2011). This behavior was an effective null model allowing for comparisons against other swimming behaviors to assess whether or not more sophisticated models perform better than random movement (Humston et al., 2004; Watkins and Rose, 2013). Random swimming was simulated by drawing a random swimming angle in the horizontal plane from a von Mises distribution. This circular normal distribution depends on two parameters, μ and κ, where μ represents the mean direction and κ represents the concentration around this direction. To simulate uncorrelated and unbiased random movement, μ and κ were both set to zero. While fish move vertically based on flows, vertical swimming was not included in the random walk behavior or other movement models.

In addition to the uncorrelated and unbiased random walk, a biased correlated random walk (BCRW) was used for yearling Chinook salmon. It differed from the uncorrelated random walk because movement at each time step was correlated to the direction of movement in the previous time step, leading to a local directional bias (Codling et al., 2008). When correlation was high, an individual maintained its heading, whereas if correlation was near zero, pathways appeared random. Correlated random walks are a popular choice for movement models, as many animals tend to move forward in a persistent manner (Codling et al., 2008). In addition to the directional persistence term, this movement model included a directional bias such that movement was directed towards downstream locations. These downstream locations may not always be fixed, and instead can be adjusted based on an individual's location (Codling et al., 2004).

Movement in the BCRW was calculated from a weighted sum of a persistence term and a navigation term according to the following equations (Bailey et al., 2018; Benhamou and Bovet, 1992):

$$\Delta x_{t+1} = x_t + \frac{L_t}{10^3}\cdot\Delta t\cdot(w\cos(\Omega_T + \phi_n) + (1-w)\cos(\theta_n + \delta_n)) \quad (4)$$

$$\Delta y_{t+1} = y_t + \frac{L_t}{10^3}\cdot\Delta t\cdot(w\sin(\Omega_T + \phi_n) + (1-w)\sin(\theta_n + \delta_n)) \quad (5)$$

where x and y are the locations, L_t is the fork length (mm), t is time, w is a weighting term, Ω_T is the target direction, Φ_n is the navigation error term, θ_n is the direction of movement in the previous step, and δ_n is a persistence error term.

Initial attempts to use the estuary mouth as a downstream target to orient fish towards when calculating the bias term were ineffective, especially in the upstream reaches of the system. Due to the sinuosity of the river as well as the system's geographic extent, multiple downstream locations were used to generate the bias term, and the specific location used was dependent on the occupied hydrogeomorphic reach (Simenstad et al., 2011). At each time step, the direction to orient for the bias term (i.e. angle between the current position and the reach's downstream location) was calculated. The persistence term was determined from the angle between the current position and the last position. The BCRW employed here therefore incorporates a rheotactic response, where the persistence term considers movement due to advection as well as powered swimming in addition to biased downstream movement. The weighting term (w) was set to 0.1 and was based on values used in Benhamou and Bovet (1992). The navigation error term and the persistence error term both used a von Mises distribution where κ, the measure of concentration around the angle of movement, equaled two.

The final movement model used for yearling Chinook salmon was a taxis behavioral response to ambient flow environments. This behavior was selected based on assumptions that yearlings time their migration to coincide with the spring freshet and typically spend less time in the estuary. Rheotaxis refers to a behavior where a fish aligns its swimming direction based on flows (Fraenkel and Gunn, 1940), and this behavior has been suggested as a strategy used by salmonids during their ocean migration (Booker et al., 2008; Burke et al., 2014; Mork et al., 2012; Royce et al., 1968) and return migrations (Hamilton and Mysak, 1986; Healey et al., 2000). Negative rheotaxis has also been suggested as a behavioral response to changing light conditions that encourages downstream movement in smolts (Cooke et al., 2011).

Negative rheotaxis describes movement where fish orient themselves to swim in the direction of the prevailing current, and positive rheotaxis describes movement where fish orient themselves to move against the current. In this case, negative rheotaxis was simulated, such that yearling Chinook salmon optimized their movement to align with the currents. In upstream reaches of the system where river flows dominate, swimming directions were associated with riverine flows. In reaches where there is greater tidal forcing, movement was more closely tied to the phase of the tide as individuals swim in the same direction that they are displaced by advection. The angle of movement was computed from the horizontal velocity vectors at the currently occupied position with random noise added using a von Mises distribution where κ equals two.

For subyearling Chinook salmon, passive and random walk

behaviors were simulated in addition to kinesis and restricted-area search swimming behaviors that depended on the expected consumption rate or growth rate. The growth rate depends on water temperatures and the *P*-value, where high values are associated with wetland habitat. The kinesis behavior entails movement that is responsive to ambient conditions but nondirectional, while the restricted-area search is more directional, with the individual assessing nearby habitat for optimal environmental conditions and moving there.

Kinesis behaviors result from an individual responding to environmental stimuli (e.g., temperature, salinity, flows) and either adjusting their speed (orthokinesis) or direction (klinokinesis) (Fraenkel and Gunn, 1940). Kinesis behaviors are a popular choice in IBMs (see Fiechter et al., 2015b; Okunishi et al., 2012; Politikos et al., 2015; Rose et al., 2015; Watkins and Rose, 2017). Swimming velocities consist of an inertial component as well as a random component, defined as:

$$V_x(t) = f_x + g_x \tag{6}$$

$$V_y(t) = f_y + g_y \tag{7}$$

In this IBM, the inertial components (f_x and f_y) were calculated as:

$$f_x = V_x(t-1)\cdot H_1\cdot I_H \tag{8}$$

$$f_y = V_y(t-1)\cdot H_1\cdot I_H \tag{9}$$

The random components (g_x and g_y) were calculated as:

$$g_x(\theta) = \Phi\cdot\varepsilon(\theta)\cdot(1 - H_2\cdot I_H) \tag{10}$$

$$g_y(\theta) = \Phi\cdot\varepsilon(\theta)\cdot(1 - H_2\cdot I_H) \tag{11}$$

Variables in the above equations represent the following: $V_x(t–1)$ and $V_y(t–1)$ are the *x*- and *y*- velocities during the last time step, I_H represents an index of habitat quality, Φ is the maximum sustained swimming speed, and $\varepsilon(\theta)$ is a unit vector of a random angle generated using the von Mises distribution. H_1 and H_2 determine the height of the function, and values used in Humston et al. (2000) and Okunishi et al. (2012) were used ($H_1 = 0.75$, $H_2 = 0.9$). Whereas most other swimming behaviors used a standard swim speed based on the assumption of 1 BL s^{-1}, this behavioral model had an evolving swim speed that depended on habitat quality. The maximum swimming speed used in this case was 4 BL s^{-1}. When the inertial component was dominant, the swimming velocities were reduced; however, when the random component was dominant, the swimming velocities were closer to the maximum swimming speed values.

The inertial and random component depended on the habitat quality (I_H) of the currently occupied element (Humston et al., 2004; Okunishi et al., 2012), which was calculated as the product of two terms:

$$I_H = I_T\cdot I_F \tag{12}$$

where I_T is a temperature dependence function used to calculate consumption in the bioenergetics model, and I_F is a metric representing prey availability. Since data on prey availability are limited for the entire estuary, I_F in this IBM was equal to the *P*-value of the occupied element that was based on the proximity to wetland habitat. Both I_T and I_F had theoretical maximums of 1. When I_H was high, movement was dominated by the inertial component, and when I_H was low, movement was dominated by the random component.

The restricted-area search behavior was slightly more complex than the kinesis behavior and consisted of an individual assessing the growth rate potential of the currently occupied element and all neighboring elements and moving to the element with the highest value (Humston et al., 2004; Railsback et al., 1999; Watkins and Rose, 2013). Other IBMs use metrics of habitat quality that are based on growth and mortality cues; however, this approach did not account for mortality. The growth rate potential for each element was calculated using the depth-averaged temperature at the element center. The direction of swimming was computed based on the angle between the fish's current position and the center of the neighboring element with the highest growth rate potential. Stochastic noise was added using a von Mises distribution where κ equals two. Velocity was computed as:

$$V_x(t) = \frac{L_i(t)}{10^3}\cdot\cos(\theta(t) + \varepsilon) \tag{13}$$

$$V_y(t) = \frac{L_i(t)}{10^3}\cdot\sin(\theta(t) + \varepsilon) \tag{14}$$

where V is the velocity (m s^{-1}), L is the body length (in mm) divided by 10^3 to convert to m, θ is the angle between the current position and destination element, and ε is stochastic noise.

For all movement models, if the trajectory computed by swimming resulted in the fish exiting the domain or getting stranded on land, the model continued to make attempts using different stochastic noise values until the trajectory resulted in the fish reaching a wet element. If fish movement resulted in vertical exit from the river, it was returned to the water surface (if exiting at surface) or to the bottom surface (if exiting at bottom). If an individual occupied an element that dried out at the next time step, it was nudged to the nearest wet element.

2.4.3.5. Growth sub-model. The bioenergetics model relates the environmental conditions experienced during migration to individual growth, allowing for an assessment of how simulated behaviors and migration pathways influence size and condition. Growth in the IBM was simulated using the Wisconsin Bioenergetics model (Hanson, 1997) with parameters for Chinook salmon defined in Table 2. Most of the original parameters described for adult Chinook salmon were used

Table. 2
Parameters, descriptions, and values used in bioenergetics sub-model based on the Wisconsin bioenergetics model. Adult parameters were used, with the exception of juvenile parameters (*) used to calculate consumption.

Parameter	Description	Value	Reference
W	Fish mass (g)	–	–
α	Allometric mass function intercept	5764.0	1
β	Allometric mass function slope	0.5266	1
	Consumption		
a_c	Allometric mass function intercept	0.303	1
b_c	Allometric mass function slope	−0.275	1
CQ	Lower temperature (°C) for C_{max}	4.97*	2
CTO	Optimum temperature (°C) for C_{max}	20.93*	2
CTM	Maximum temperature (°C) for C_{max}	20.93*	2
CTL	Upper temperature (°C) for C_{max}	24.05*	2
CK_1	Proportion of C_{max} at CQ	0.09*	2
CK_4	Proportion of C_{max} at CTL	0.53*	2
	Respiration		
a_r	Allometric mass function intercept	0.00264	1
b_r	Allometric mass function slope	−0.217	1
RQ	Approximates Q_{10}	0.06818	1
RTO	Coefficient of swimming speed	0.0234	1
SDA	Specific dynamic action	0.172	1
	Egestion (F) and Excretion (U)		
a_f	Intercept of the proportion of consumed energy egested versus water temperature and ration	0.212	1
b_f	Coefficient of water temperature dependence of egestion	−0.222	1
g_f	Coefficient for feeding level dependence (*P*-value) of egestion	0.631	1
a_u	Intercept of the proportion of consumed energy excreted versus water temperature and ration	0.0314	1
b_u	Coefficient of water temperature dependence of excretion	0.58	1
g_u	Coefficient for feeding level dependence (*P*-value) of excretion	−0.299	1

[1]Stewart and Ibarra (1991).
[2]Plumb and Moffitt (2015).

(Stewart and Ibarra, 1991), with the exception of the temperature-dependent consumption parameters that were more recently defined for subyearling Chinook salmon (Plumb and Moffitt, 2015).

Weight (W) was computed according to the following:

$$W_t = W_{t-1} + [C - (R + S + F + U)]\cdot\frac{e_p}{e_f}\cdot W_{t-1} \quad (15)$$

where C is consumption, R is respiration, S is specific dynamic action, F is egestion, and U is excretion, with C, F, and U in units of g prey g fish $^{-1}$ d^{-1}, and R in units of g O_2 g fish^{-1} d^{-1}. Variables e_p and e_f represent the prey energy density and the fish energy density. Each of these variables was computed from temperature- and mass-dependent functions. While reproduction is often included in this bioenergetics model, it was not considered in this application. The equations used in the Wisconsin Bioenergetics model were originally intended for a daily time step; however, growth in the IBM was computed every 15 min, thus the final growth term was divided by 96.

Consumption was calculated according to:

$$C = C_{max}\cdot p\cdot f(T) \quad (16)$$

$$C_{max} = a_c\cdot W^{b_c} \quad (17)$$

where C is the specific consumption rate (g g^{-1}d^{-1}), C_{max} is the maximum specific feeding rate (g g^{-1} d^{-1}), p is the proportion of maximum consumption, $f(T)$ is a temperature dependence function, T is water temperature (°C), W is fish mass (g), a_c is the intercept of the allometric mass function, and b_c is the slope of the allometric mass function. The temperature dependence function used in this application was Eq. (3), temperature dependence for cool- and cold-water species (Thornton and Lessem, 1978). This function was also used in the kinesis model when calculating habitat quality.

Respiration, the energy used for routine metabolism, depends on the water temperature and the fish's size and activity. The total metabolism includes routine metabolism and digestion (i.e., specific dynamic action (SDA)). Energy lost to respiration was determined by multiplying the mass-dependent resting metabolism component by a temperature dependence function and activity component:

$$R = a_r\cdot W^{b_r}\cdot f(T)\cdot Activity \quad (18)$$

where R is respiration (g g^{-1}d^{-1}), a_r is the intercept of the allometric mass function, W is weight (g), b_r is the slope of the allometric function, $f(T)$ is a temperature dependence function, and *Activity* is an activity multiplier that depends on the swimming speed (cm s^{-}1) of the fish. The temperature dependence function used in the IBM was Eq. (1), exponential with swimming speed (Stewart et al., 1983). While the velocity used in the kinesis model was variable, an approach similar to that used in Humston et al. (2004) was used such that *vel* is set to 1 BL s^{-1}. Since the effect of swimming velocity on metabolism was less important than the effect of swimming behavior on simulated estuarine migration pathways and residence times, this helped to eliminate differences across the subyearling Chinook salmon movement models. SDA is equal to a proportion of energy consumed and was calculated according to:

$$S = SDA\cdot(C - F) \quad (19)$$

Egestion (F) and excretion (U) depend on mass, temperature, and ration (Elliott, 1976) and were calculated as follows:

$$F = a_f\cdot T^{b_f}\cdot e^{\left(g_f\cdot p\right)}\cdot C \quad (20)$$

$$U = a_u\cdot T^{b_u}\cdot e^{(g_u\cdot p)}\cdot(C - F) \quad (21)$$

where a_f is the intercept of the proportion of consumed energy egested versus water temperature and ration, b_f is the coefficient of water temperature dependence of egestion, and g_f is the coefficient for feeding level dependence of egestion. Variables a_u, b_u, and g_u are similarly defined but for excretion.

Outputs from the bioenergetics equations were converted from units of g g^{-1} d^{-1} to units of J g^{-1} d^{-1} by multiplying consumption (C), egestion (F), and excretion (U) by the prey energy density. Prey energy densities were based on a common prey type of juvenile Chinook, chironomid pupae (Diptera), for which typical energy densities are 3400 J g^{-1} (Koehler et al., 2006). Respiration was also converted to units of (J g^{-1}d^{-1}) by applying the oxy-calorific coefficient (13,560 J g^{-1} O_2) to convert the oxygen consumed to energy consumed (Hanson, 1997; Stewart et al., 1983). Once units were converted, growth in g d^{-1} was calculated by dividing by the fish energy density and multiplying by the mass of the fish. Energy density was calculated as:

$$e_f = \alpha + \beta\cdot W \quad (22)$$

where e_f is the fish energy density (J g^{-1}), α is the intercept of the allometric mass function, β is the slope of the allometric mass function, and W is the fish mass (g).

To obtain the weight of the fish at each time step, the computed growth was added to the weight at the previous time step. Depending on whether or not loss terms were greater than consumption terms, the fish either lost or gained weight. Data on subyearling and yearling Chinook salmon fork lengths from the lower estuary were used to generate a weight-length relationship equation, and this equation was then used to compute fork length from the new weight. Increases in length due to weight gain were calculated according to:

$$W = aL^b \quad (23)$$

where W is the mass of the fish (g), a is the intercept, L is the length (mm), and b is the slope. The slope and intercept were determined using observed length-weight data, and Eq. (23) was rearranged to solve for L:

$$L = \left(\frac{W}{e^{-12.27476}}\right)^{\frac{1}{3.18421}} \quad (24)$$

Although fish weight can fluctuate, their length cannot decrease as their weight decreases. Thus, a fish was only allowed to increase in length if it was greater or equal to the expected weight for a fish of its size. If the weight was greater or equal to this expected value, the fish increased in length; however, if the weight was less than this expected value, its length remained the same.

2.5. Analysis

To assess the skill of the passive particle tracking model, particles were simulated in a forward pattern during low and high flow periods for one, two, and three days. The tracks generated by the forward particle tracking were compared against backward tracks that were initialized from the final positions of the forward tracks. To evaluate skill, the distances between the starting positions from the forward tracking and final positions from the backward tracking were computed. The two periods simulated were a low flow period in April and a high flow period in June, corresponding with the freshet. Simulations were conducted for various lengths of time to explore how the simulation length and distances traveled impacted model skill.

Results from yearling and subyearling Chinook salmon simulations were analyzed by describing estuarine residence times, travel times to various locations throughout the estuary, and growth. Model results were compared against observed travel times from the pair trawl as well as travel times from JSATS data. The comparison between simulated migration timing and observed migration timing was done by comparing bulk statistics, and it should be noted that direct comparisons between model results and observations were not achievable in this application. There were also temporal differences between the observations and the model results. The timing of the pair-trawl experiment (March 23 through August 4) differed from the timing of

individual initializations at Bonneville for yearling Chinook salmon (March 13–July 5) and subyearling Chinook salmon (April 25–September 4), but despite this, all individuals were considered as there was not significant variability in travel times to Jones Beach over time. JSATS data collection did not commence until late April. Since the observed detections at the JSATS arrays occurred from April 29–June 15 for yearling Chinook salmon and June 14–August 15 for subyearling Chinook salmon, only simulated fish that were active in the estuary during these periods were considered in model-data comparisons with the JSATS data. Lastly, the subyearling Chinook salmon targeted in the JSATS study were larger than simulated subyearling Chinook salmon, but this size difference was not accounted for in the analysis.

In addition, results from simulations were analyzed by visualizing common migration pathways and comparing against migration pathways described in Harnish et al. (2012). The impacts of environmental conditions on potential estuarine migration pathways were explored by analyzing the estuarine residence times against river flows at initialization and the tides at the time of marine entry. The effects of swimming behaviors were explored with a greater emphasis on how behaviors of varying complexity influence migration patterns and travel rates and how they compare with observations and less on identifying the correct mechanisms that control behavioral decision-making. The IBM was intended to be used as an exploratory tool to assess the efficiency of behavioral mechanisms on simulating potential migration pathways of different life-history types. Comparisons of more sophisticated movement models against passive and random walk simulations made it possible to determine if simple swimming behaviors and/or passive drift adequately simulated migration histories or if more complex behaviors were appropriate.

Data from the 2010 pair-trawl study as well as PIT-tag detections from Bonneville Dam were downloaded from PTAGIS. As there were often multiple detections of a single tag at one monitoring location, the last record was used, such that each tag only had one unique result at each location. Data from Bonneville Dam juvenile stations and the pair trawl (TWX) were joined using the tag code identification number, and the travel time to Jones Beach was computed by subtracting the time of detection at Bonneville from the time of detection by the pair trawl. Travel times to Jones Beach for simulated fish were determined by calculating the time at which individuals passed -123°16′ 50.541″, the approximate longitudinal location of Jones Beach (Fig. 1).

JSATS data were downloaded from JSITE, and travel times between cross-channel arrays were computed for rkm 86–50, rkm 50–37, rkm 37–22, and rkm 22–8. At each upstream array, the time of last detection was computed for all individuals, and at each downstream array, the time of first detection was calculated. In instances where individuals were detected by both the navigation channel array and peripheral channel array in the same general longitudinal location (e.g., rkm 50, rkm 37, rkm, 22, rkm 8), individuals were assigned to the upstream array where the last detection occurred. When computing the time of first detection at the downstream array, it was therefore necessary to factor in the time of last detection at the upstream array to ensure that all travel times reflected downstream movement. Prior to this consideration, some of the travel times between downstream and upstream arrays were negative because the tides would transport fish near the estuary mouth back into the estuary and past the upstream array where it was already detected. Since a fish may have passed an upstream array multiple times due to the tides, it was necessary to account for this pattern of movement when computing first and last detection times. In addition, the time of detection at the downstream array considered all detections for that unique rkm (e.g., rkm 50, 37, 22, and 8), and did not distinguish between the main or navigation channel. This method was implemented for both the JSATS data and simulated fish. For a more detailed description of how JSATS travel times and pathways were calculated, see Harnish et al. (2012).

Table. 3
Mean and standard deviation of passive particle tracking skill and mean distances traveled during low and high flow periods.

Simulation Length (days)	Flows	Model skill (m)	Distance traveled (km)
1	Low	0.16 ± 0.38	54.4
1	High	1,122.28 ± 1,455.12	104.6
2	Low	0.16 ± 0.39	96.0
2	High	9,045.68 ± 8,542.73	191.8
3	Low	153.29 ± 1,377.06	142.4
3	High	11,367.60 ± 19,003.91	239.0

3. Results

3.1. Particle tracking skill

Errors in particle tracking can potentially distort simulated migration pathways in significant ways. To assess tracking skill, we used a closure approach, where once a forward track was concluded, we backward track from the end position to reconstruct the starting position at the starting time. The distance between the original and reconstructed starting positions should be zero. The larger the distance is, the lesser the skill.

During low flow periods, the particle tracking skill was high, especially when only one or two days were simulated (Table 3). The mean skill was 0.16 ± 0.38 (0.39) m for the one-day and two-day low flow simulations. Model skill decreased as the simulation length increased, with the mean distance between the starting forward positions and final backward positions increasing to 153.29 ± 1377.06 m. The particle tracking skill was also less during the high flow period, where error was several orders of magnitude greater than the error during low flow periods with mean values ranging from 1122.28 m for the one-day simulation up to 11,367.60 m for the three-day simulation. Distances traveled were much greater during the high flow periods, and were often twice as much as the distances traveled during low flow periods, especially in the upper reaches of the river. With the increases in flows and distances traveled, the likelihood of particles exiting the domain was higher during the high flow period, which could allow small errors in trajectories to be propagated over time when conducting backtracking. In addition, during the high flow period, there were more particles that entered the ocean, and backtracking from these initial positions could further introduce large errors, especially if the particles did not return to the estuary.

3.2. Travel times, residence, and migration pathways

3.2.1. Travel times

Travel times were considered for multiple regions, including the upper estuary between Bonneville Dam and Jones Beach, the region sampled by the pair trawl. Travel times and migration pathways were also described for the lower estuary, between rkm 86, and various locations in the main channel and peripheral channels at rkm 50, 37, 22, and 8.

Travel times to the pair-trawl and between JSATS arrays were right-skewed and not normally distributed, so median values are described. In addition, means and standard deviations are reported in Table 4 for reference. The median travel time for yearling Chinook salmon observed in the pair-trawl experiment was 2.00 days (n = 3632). Across all yearling Chinook salmon simulations, median travel times to Jones Beach ranged from 2.10 to 2.49 days (Table 4, Fig. 5), with values of 2.40 days for the passive particle simulation, and 2.49 for the random walk simulation. The more complex yearling Chinook salmon behaviors, including negative rheotaxis and biased correlated random walk resulted in reduced median travel times of 2.17 and 2.10 days.

Table. 4
Results of model simulations for yearling and subyearling Chinook salmon swimming behaviors, including the mean (μ), standard deviation (σ), and median ($\tilde{x}$) values for various run metrics. Values reported include the travel time to Jones Beach (days), estuarine residence time (days), the daily distance traveled (km d^{-1}), and the daily growth (mm d^{-1}) for all individuals that successfully exited the estuary.

	Travel time to Jones beach (days)		Estuarine residence time (days)		Daily distance traveled (km d^{-1})		Daily growth (mm d^{-1})	
Yearling	μ ± σ	$\tilde{x}$	μ ± σ	$\tilde{x}$	μ ± σ	$\tilde{x}$	μ ± σ	$\tilde{x}$
Passive	2.37 ± 0.53	2.40	5.37 ± 1.95	5.11	56.08 ± 9.26	55.87	–	–
Random walk	2.54 ± 1.34	2.49	5.80 ± 2.78	5.38	53.54 ± 9.83	53.48	0.19 ± 0.07	0.20
Taxis	2.21 ± 1.18	2.17	5.18 ± 1.93	4.92	61.19 ± 9.97	61.11	0.19 ± 0.07	0.20
BCRW	2.12 ± 0.92	2.10	5.09 ± 2.02	4.78	61.24 ± 10.37	61.27	0.19 ± 0.07	0.20
Subyearling								
Passive	2.26 ± 1.80	2.23	5.56 ± 6.30	4.83	59.53 ± 12.48	58.83	–	–
Random walk	2.33 ± 1.13	2.27	5.90 ± 7.11	4.96	58.12 ± 13.30	57.08	0.30 ± 0.06	0.30
Kinesis	2.48 ± 1.05	2.39	6.65 ± 8.55	5.24	55.12 ± 13.52	54.86	0.33 ± 0.07	0.33
Area Search	7.35 ± 15.49	3.04	22.51 ± 25.98	9.34	32.33 ± 17.95	33.51	0.52 ± 0.14	0.48

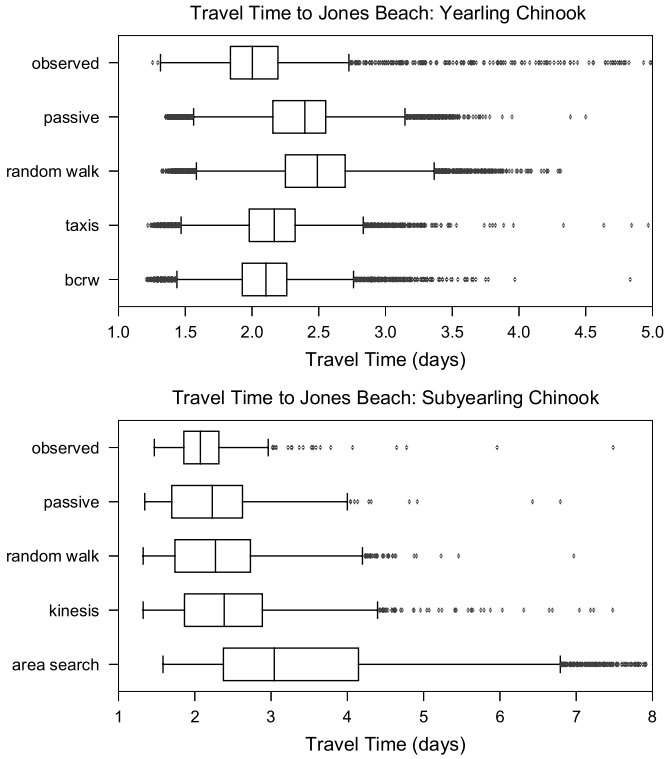

Fig. 5. Yearling Chinook salmon (*top*) and subyearling Chinook salmon (*bottom*) travel times to Jones Beach, including observations from the pair-trawl experiment and simulated fish employing different movement models.

Median travel time from the pair trawl experiment for subyearling Chinook salmon detected from March 23 through August 4 was 2.07 days (n = 461). The simulated travel times to Jones Beach for subyearling Chinook salmon were slightly longer than observed values and were fairly similar to those of yearling Chinook salmon (Table 4, Fig. 5). Median travel times from the passive and random walk simulations were 2.23 and 2.27 days. Fish simulated using the kinesis behavior had a median travel time of 2.39 days. Travel times for the restricted-area search behavior were longer than the other movement model travel times, with a median value of 3.04 days. This behavior was also much more right-tailed than the others. While there was a discrepancy in the temporal overlap between observed and simulated data, overall, there was very little difference between the observed yearling Chinook salmon travel times and subyearling Chinook salmon travel times from the pair trawl. It's also important to note that the sample sizes between the two were not equivalent and that yearling Chinook salmon were the life-history type of interest during the pair-trawl experiments.

In general, the median travel times to Jones Beach from the IBM were consistently greater than median observed travel times to Jones Beach; however, this difference in travel times was on the scale of hours. For both the yearling and subyearling Chinook salmon passive simulations, travel times due to passive drift were fairly close to the median observed travel times. This suggests that passive drift alone could be largely responsible for travel times through upstream reaches of the system, and that swimming behavior, while important, may not be as important of a driver. However, it's also important to note that the passive behavior was not as right-skewed as the observations, suggesting that passive drift does not capture the variability in travel times that is more evident in the observations and active swimming behaviors.

Travel times for yearling and subyearling Chinook salmon from Harnish et al. (2012) as well as simulated travel times across behaviors are described for various segments of the lower estuary in Table 5 and shown in Figs. 6 and 7, with the array locations shown in Fig. 1. In general, travel times for simulated yearling and subyearling Chinook salmon were within several hours of the observed travel times. Most simulated travel times were several hours longer than the observed travel times, with the exception of the travel times between the navigation channel at rkm 50 to rkm 37 and the north channel near the Washington shoreline between rkm 22 and rkm 8. Travel times from Clifton Channel (CC50) to rkm 37 were much greater for simulated yearling and subyearling Chinook salmon, with the exception of the biased correlated random walk behavior.

The median observed travel times between the navigation channel at rkm 86 and rkm 50 for yearling and subyearling Chinook salmon were 12.4 and 12.2 h. Simulated median travel times for yearling and subyearling Chinook salmon between these points ranged from 14.9–17.4 h and 15.2–17.2 h. Median observed travel times for yearling and subyearling Chinook from the navigation channel at rkm 50 to rkm 37 were 4.5 and 5.1 h, while simulated median travel times ranged from 3.0–3.6 h for yearling Chinook salmon and 3.3–7.9 h for subyearling Chinook salmon. The travel times from Clifton Channel (CC 50) to rkm 37 were often twice as long for simulated Chinook salmon. In addition, the proportion of simulated fish detected in Clifton Channel was much less than the proportion of observed juvenile Chinook salmon detected in this peripheral channel.

From the navigation channel at rkm 37 to rkm 22, the median observed travel times for yearling and subyearling Chinook salmon were 11.9 h and 12.7 h. For the passive and random walk yearling behaviors, simulated travel times in this reach were nearly twice as long as

Table. 5
Median travel times (hours) in the lower estuary between cross-channel JSATS arrays located in main and peripheral channels. Main channels are denoted with the Nav prefix, and peripheral channels are denoted with acronyms CC (Clifton Channel), CB (Cathlamet Bay) and WA (Washington shoreline).

	Nav86 to rkm50	Nav50 to rkm37	CC50 to rkm37	Nav 37 to rkm 22	CB37 to rkm 22	Nav 22 to rkm 8	WA 22 to rkm 8
	Yearling Chinook Salmon						
Literature[1]	12.4	4.5	12.1	11.9	9.3	2.8	2.2
Observed[2]	12.5	4.5	12.1	11.9	9.3	2.8	2.2
Passive	16.2	3.5	24.3	21.3	12.7	6.4	2.0
RW	17.4	3.6	26.9	21.9	13.4	7.0	2.0
Taxis	14.9	3.0	25.0	15.0	12.4	3.9	2.0
BCRW	14.9	3.0	16.2	14.7	12.6	3.7	1.9
	Subyearling Chinook Salmon						
Literature[1]	–	5.1	11.9	12.7	10.3	4.0	2.1
Observed[2]	12.2	5.1	11.9	12.7	10.3	4.0	2.1
Passive	15.2	3.3	–	16.9	13.2	3.6	1.9
RW	15.4	3.4	29.4	17.0	13.3	4.4	1.9
Kinesis	15.8	3.6	28.4	16.9	13.5	9.4	2.0
Area search	17.2	7.9	27.6	26.1	22.8	4.9	2.0

[1] Values reported in Harnish et al. (2012) study.
[2] Observed values are calculated from JSATS data downloaded from JSITE. These same values are portrayed in Figs. 6 and 7.

observed values, while the travel times for the negative taxis and biased correlated random walk behaviors were approximately three hours longer. The simulated travel times for subyearling Chinook salmon were up to four hours longer in this reach, with the exception of the area search behavior that was over twice the observed rate. From Cathlamet Bay at rkm 37 to rkm 22, observed travel times were 9.3 and 10.3 h, and most simulated behaviors for yearling and subyearling Chinook salmon were approximately three hours longer, except the area search behavior.

Median travel times from the navigation channel from rkm 22 to rkm 8 were 2.8 and 4.0 h for observed yearling Chinook salmon and subyearling Chinook salmon. The simulated travel times for the passive and random walk yearling Chinook salmon behaviors through this reach were several hours longer, while those of the negative taxis and biased correlated random walk behaviors were just over an hour longer. For simulated subyearling Chinook salmon in this reach, the median travel times for the passive, random walk, and area search behaviors were within minutes to an hour of the observed travel times, while the time of the kinesis behavior was over twice as long. The median travel times between rkm 22 along the Washington side (WA 22) to rkm 8 were 2.2 and 2.1 h for observed yearling and subyearling Chinook salmon, and median simulated times ranged from 1.9–2.0 h for yearling and subyearling Chinook salmon. Within this region, median simulated travel times were nearly identical to the median observed times, and there was very little variation across the behaviors, suggesting that behavioral effects in this region were minimal and that physical processes dominate.

In general, the travel times for simulated yearling Chinook salmon were consistently reduced for the negative rheotaxis and biased correlated random walk behaviors compared to the passive and random walk behaviors. In the rkm 50 to rkm 37 reach, the simulated travel times for both yearling and subyearling Chinook salmon were less than observed travel times. The behavior that stood out as the most variable from observations was the restricted-area search because of the longer travel times between arrays.

3.2.2. Estuarine residence times

Estuarine residence times for yearling Chinook salmon did not vary significantly across the different swimming behaviors (Table 4, Fig. 8). In the passive particle simulation, the median time to estuarine exit was 5.11 days, and the median distance traveled per day was 55.87 km. The random walk behavior resulted in slightly longer estuarine residence times of 5.38 days and a slightly decreased rate of travel of 53.48 km d^{-1}. The median estuarine residence times of the negative rheotaxis and biased correlated random walk were slightly decreased at 4.92 and 4.78 days respectively, with median travel rates of 61.11 and 61.27 km d^{-1}. This difference in distances traveled between the passive and random walk simulations and the more sophisticated behaviors was due to the behavioral response of orienting movement based on the direction of prevailing currents and resulting directional biases.

Median estuarine residence times for simulated subyearling Chinook salmon were close to simulated yearling Chinook salmon estuarine residence times, and with the exception of the restricted-area search behavior, did not differ significantly across swimming behaviors (Table 4, Fig. 8). Median estuarine residence times were 4.83 days for the passive behavior, 4.96 days for the random walk behavior, 5.24 days for the kinesis behavior, and 9.34 days for the restricted-area search behavior. The median distance traveled per day in the restricted-area search behavior (33.51 km d^{-1}) was significantly less than the distances traveled in the simpler behavioral models and kinesis model (54.86–58.83 km d^{-1}). While the medians were more appropriate to report as the data were not normally distributed, the variability in subyearling Chinook salmon estuarine residence times was especially evident when comparing the means and standard deviations. The restricted-area search behavior mean residence time and standard deviation were between 3–4 times greater than the other behaviors, with values of 22.51 ± 25.98 days. Longer estuarine residence times are typical for subyearling Chinook salmon, so longer estuarine residence times observed in the restricted-area search behavior suggest that swimming behavior can have an important influence on residence times.

Flow magnitude largely influenced simulated estuarine residence times for both yearling and subyearling Chinook salmon (Fig. 9), and this was especially evident for the yearling Chinook salmon behaviors, passive particle simulations for both yearling and subyearling Chinook salmon, and the random walk and kinesis behaviors for subyearling Chinook salmon. For the restricted-area search behavior, estuarine residence times were mostly reduced when river discharge at the time of release was greater than ~8000 $m^3 s^{-1}$, and when flows were less than this threshold, residence times were much longer. The phase of the tide also impacted the timing of marine entry, as most yearling and subyearling Chinook salmon exited the estuary during the ebb phase (Fig. 10). For several of the behaviors (e.g., negative rheotaxis, and biased correlated random walk), this behavior was built in, as fish oriented their swimming direction to move in the direction of prevailing currents. However, even for behaviors where swimming was not based on the flow direction, most fish exited during the ebb phase. Since flow velocities in the lower estuary were high when both river discharge and tidal velocities directed flows seaward, fish movement would be largely driven by advection and behavioral effects would likely be insignificant.

3.2.3. Migration pathways

Migration pathways were analyzed across simulated yearling and subyearling Chinook salmon behaviors by examining the common routes used, with a particular emphasis on the lower estuary. In general, yearling Chinook salmon migration pathways were concentrated in the navigation channel, before passing through the tidal flats into the north channel (Fig. 11). There was minimal transport into the lateral bays in the passive simulation, with the exception of Baker Bay. Migration pathways for the random walk simulation did not differ much from the passive particle pathways, although there were slightly greater

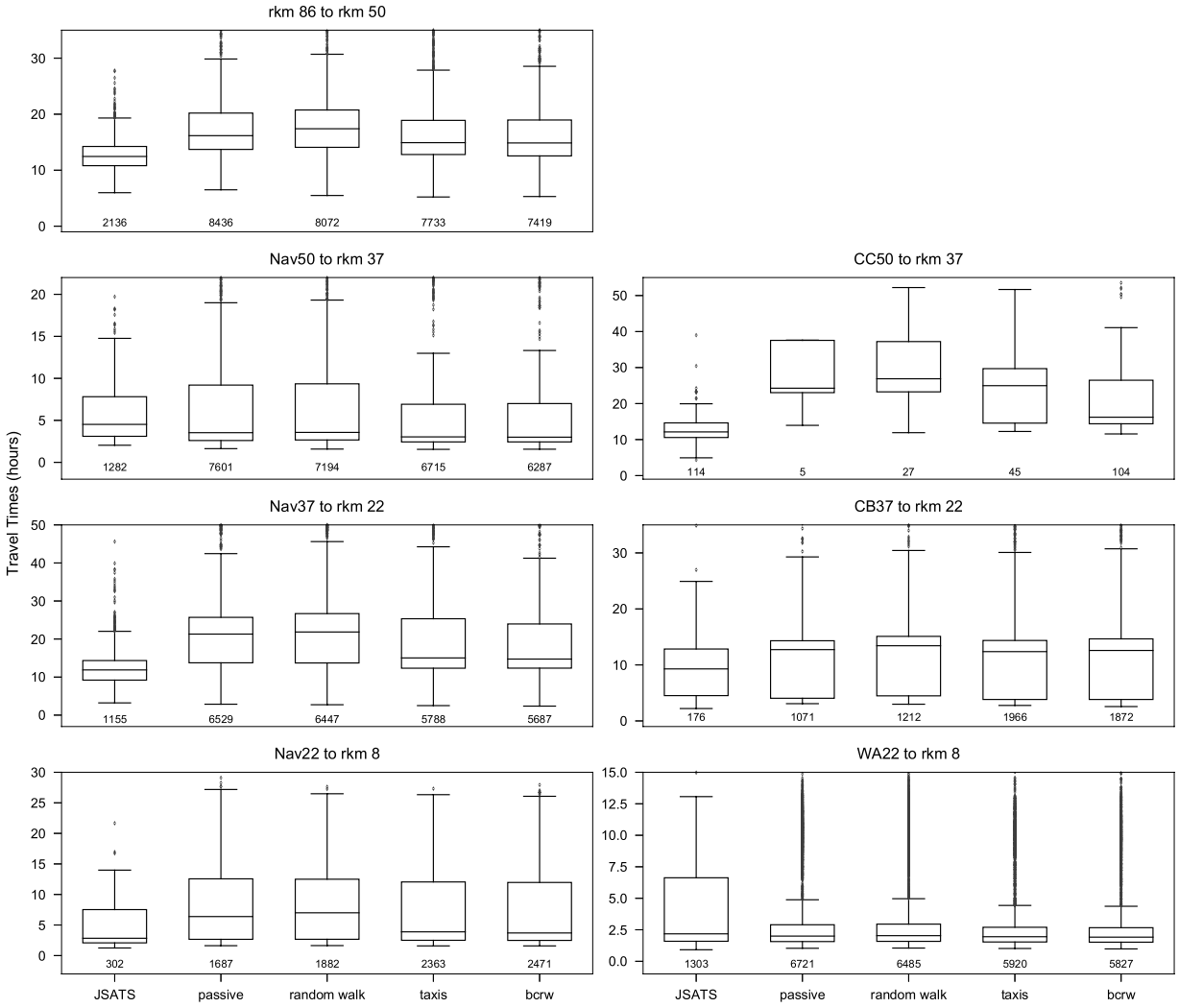

Fig. 6. Yearling Chinook salmon travel times (hours) between the JSATS arrays for observed and simulated fish. Only simulated fish detected from April 29–June 15, 2010 are represented to correspond with observed dates. The number of individuals described is indicated ibelow the boxplots.

concentrations in the lateral bays.

In the more complex yearling Chinook salmon behaviors, negative rheotaxis and the biased correlated random walk, individuals were concentrated in the navigation channel and the north channel. While patterns were fairly similar to those seen in the passive and random walk simulations, there was less concentration in the tidal flats and accumulation in Baker Bay, and greater presence in Cathlamet Bay. Lastly, most individuals near the estuary mouth traveled from the north channel as opposed to the navigation channel at rkm 22, suggesting that fish move from the navigation channel across the tidal flats to the north channel.

Migration pathways for the subyearling Chinook salmon passive and random walk behaviors showed similar patterns to the yearling Chinook salmon behaviors, with pathways concentrated in the navigation channel, across the tidal flats, and in the north channel (Fig. 12). The kinesis behavior also showed concentrated migration pathways in these regions in addition to Cathlamet Bay. There were some regions in Youngs Bay and Cathlamet Bay where individuals simulated using the kinesis behavior accumulated, suggesting that flows in these regions were minimal, and the connectivity across wet elements was reduced.

Migration pathways for the restricted-area search behavior differed drastically from the other subyearling Chinook salmon behaviors. Since individuals were directed to regions with high growth rate potential, pathways for this behavior were predominantly in shallow regions of the lower estuary and the lateral bays in particular. These habitats were used more extensively than the navigation channel, which helps to explain the longer residence times using this behavior as well as the minimal distances traveled on average, when compared to other subyearling Chinook salmon behaviors.

3.2.4. Growth

Daily growth was similar across the different yearling Chinook salmon swimming behaviors with median values of 0.20 mm d^{-1} (Table 4). While most individuals grew throughout the simulation, some simulated yearling Chinook salmon did not increase in fork length at all. Minimal differences in simulated growth rates across these behaviors were likely due to the similar temperatures experienced by migrating individuals, especially since most simulated yearling Chinook salmon remained in the main channel regions and had similar travel times through the lower estuary. Even though the estuarine residence times for some of the subyearling Chinook salmon behaviors (e.g., random walk, kinesis) were fairly similar to the yearling Chinook salmon estuarine residence times, daily growth was often greater, with median values ranging from 0.30–0.33 mm d^{-1} (Table 4). This was most likely due to differences in temperatures based on the timing of the simulations, where subyearling Chinook salmon experienced warmer temperatures throughout their migration.

The restricted-area search behavior simulated for subyearling Chinook salmon resulted in the highest median growth rate of 0.48 mm d^{-1}. Individuals simulated under the kinesis behavior had

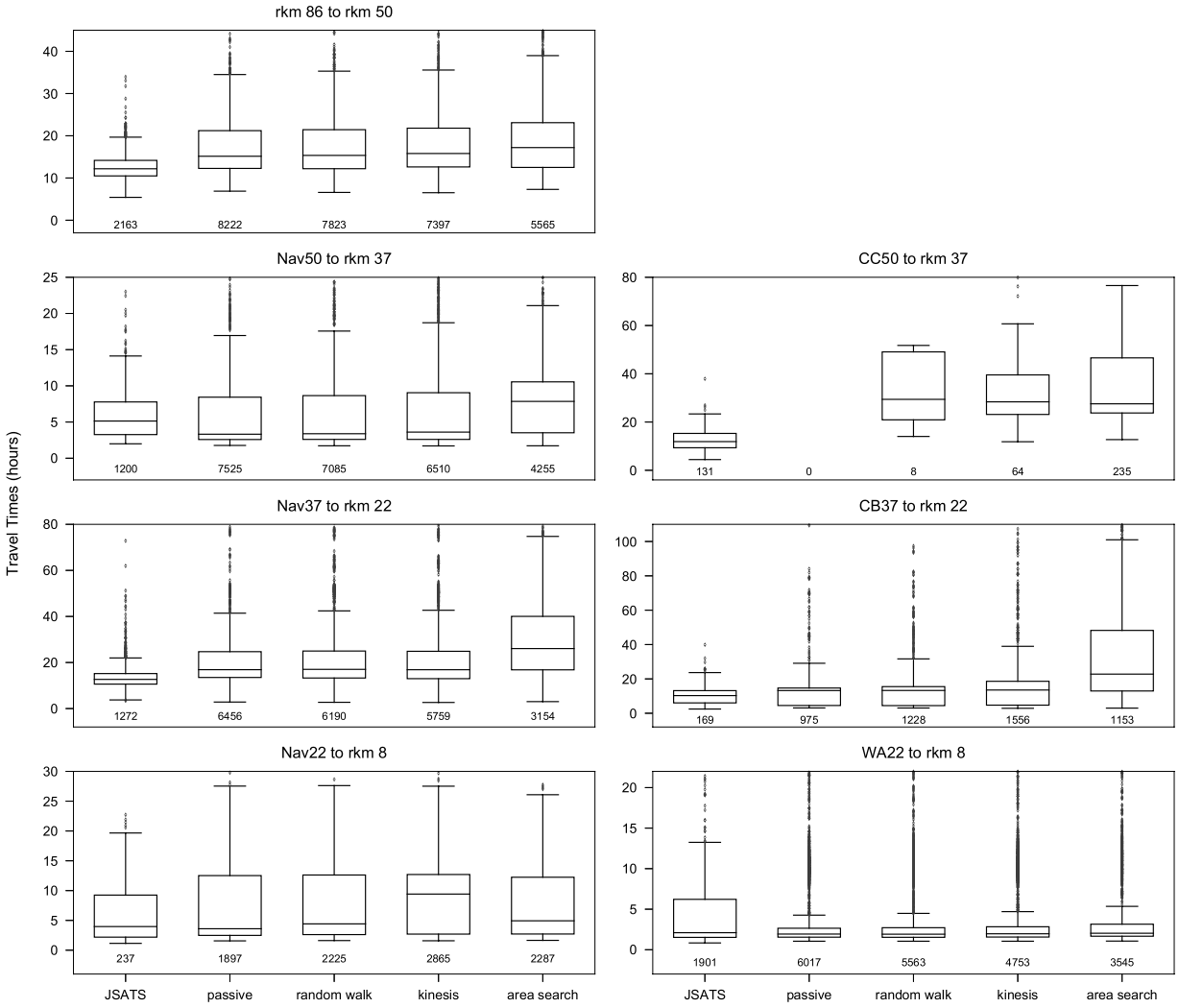

Fig. 7. Subyearling Chinook salmon travel times (hours) between the JSATS arrays for observed and modeled fish. Only simulated fish detected from June 14–August 5, 2010 are represented to correspond with observed dates. The number of individuals described is indicated below the boxplots.

slightly greater growth rates than the random behavior; however, growth rates were still less than the area search behavior. Although both the kinesis and restricted-area search behavior were designed to optimize growth, the kinesis behavior was more reactive to environmental conditions experienced, while the restricted-area search behavior had a directional bias to move to regions with the highest growth rate potential. This directional bias resulted in greater time spent in optimal temperatures and habitats, resulting in greater growth.

4. Discussion

Results from the simulations indicate that estuarine residence times are strongly influenced by riverine flow. Previous work that quantified nursery habitat for the Columbia River estuary found river forcing to be a dominant driver, while the tides were a predominant force in lower reaches (Rostaminia 2017). Across all simulated behaviors for yearling and subyearling Chinook salmon, estuarine residence times were less when flows were greater ($\sim>$ 8000 m^3/s). During periods of high discharge, estuarine residence times were mostly on the order of days. These results are consistent with those of Kärnä and Baptista (2016b), that show residence times being on the order of days in the system.

The different simulated yearling Chinook salmon behaviors did not show significant variability in travel times to Jones Beach or estuarine residence times. However, the more complex swimming behaviors that factored in directional and navigational biases and/or the direction of the prevailing currents resulted in reduced travel times and estuarine residence. This highlights the influence of swimming behavior for yearling Chinook salmon, in that some behaviors optimize movement to remain in the main channels and outside of peripheral channels. Evidence of simulated yearling Chinook salmon present in Cathlamet Bay across the movement models suggests that once juveniles enter the lower estuary, they are no longer confined to main channels and instead may move into lateral bays, both due to environmental forcing and swimming behavior. The presence of yearling Chinook salmon in Cathlamet Bay also suggests that they may utilize wetland habitats and may be directed to these regions both through advective processes and swimming behavior. This supports recent work that has challenged the existing paradigm that yearling Chinook salmon do not utilize wetland habitats.

Across the subyearling Chinook salmon swimming behaviors, there was little variability across the passive, random walk, and kinesis behaviors. However, the restricted-area search behavior differed significantly from those behaviors, leading to longer estuarine residence, increased growth, and decreased daily travel rates. The longer residence times, increased growth, and shorter distances traveled were likely associated with the occupation of peripheral habitats and lateral bays (e.g. Cathlamet Bay), where waters tend to be older (Kärnä and Baptista, 2016b). By occupying waters where flows are reduced, individuals are less likely to be rapidly flushed, and thus their estuarine residence times may be extended. In addition, individuals were more

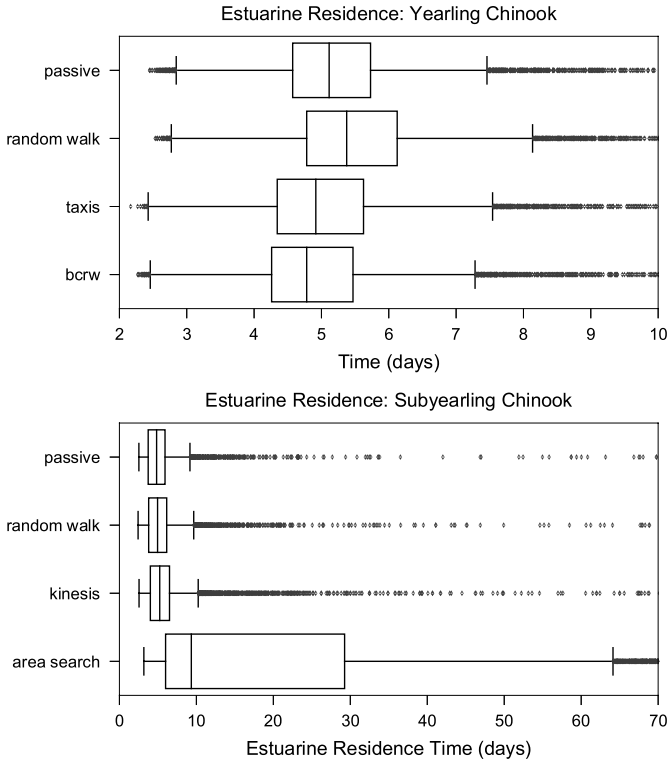

Fig. 8. Yearling Chinook salmon (*top*) and subyearling Chinook salmon (*bottom*) estuarine residence times (days) for all simulated behaviors.

likely to occupy shallower habitats where temperatures and the availability of food resources derived from wetland habitat were more optimal for growth.

Although the restricted-area search behavior was effective at directing individuals to productive shallow habitats, it often resulted in aggregation in regions of local optima. While this positively contributed to growth, once individuals occupied an area where potential growth rates were high, there was no incentive to search for new habitat. In most cases, flow velocities and randomness in the swimming behavior would limit long-term aggregation; however, in regions with frequent wetting and drying, where flows were minimal, fish could easily be artificially retained.

Previous attempts at developing a restricted-area search behavior used different criteria based on nursery habitat that was computed from depth, velocity, salinity, and temperature criteria, but these habitats were extremely patchy. Directing individuals to these regions without secondary cues resulted in minimal occupation of optimal habitats. Using a secondary cue of searching for shallow habitat was effective in directing individuals to regions with good nursery habitat, but frequently resulted in significant stranding because once fish encountered shallow habitat, they tended to stay there. In these regions, water velocities were reduced, and therefore fish moved less due to advection. Their swimming behavior became more of a driving force. When the behavior directs individuals to local optima, there is nothing to prompt movement outside of the optima, especially if flows remain low. This was also an issue when using the growth-rate potential; however, there were a lot fewer fish that got stuck in extremely shallow habitats under this method. Additional behaviors were attempted to keep individuals from getting stuck, yet they remained ineffective in leading individuals to exit the estuary.

There are several large-scale drivers that influence migration behavior, including some genetic component that entices individuals to move. While individuals may spend various amounts of time in good habitat, eventually they will be prompted to exit the estuary. Although the restricted-area search behavior was effective at reproducing expected distributions of subyearling Chinook salmon in shallow habitats, it was not effective for simulating departure from these optimal habitats, and thus may be limited when simulating a migratory species that exits the system. Future attempts should consider using a size-dependent, time-dependent, or duration-dependent behavior within the restricted-area search behavior to avoid accumulation in certain regions. While it was expected that the kinesis simulations might increase the likelihood of fish encountering wetland habitat, the reduced residence times for this simulation suggest that was not the case.

With regards to observed estuarine residence times, there have not been many studies that have documented travel times between Bonneville Dam and the estuary mouth, as most studies have focused on particular reaches of the estuary (e.g., Bonneville Dam to Jones Beach). Carter et al. (2009) found that smolts pass through the estuary more quickly during periods of high discharge and later in the migration season and that yearling Chinook salmon migrate at rates of ~60 km/day between Vancouver, Washington and the estuary mouth. These results correspond with results for simulated yearling Chinook salmon, where individuals that migrate later and during periods of high discharge have shorter estuarine residence times, and average distances traveled are on the order of 55–65 km d^{-1}. McComas et al., 2008 found that acoustic-tagged subyearling Chinook salmon moved quickly through the system to the river mouth with a mean travel time of 4.1 days. This is fairly close to the estuarine residence times of the simpler simulated subyearling Chinook salmon behaviors (e.g., passive, random walk, and kinesis).

When comparing the observed travel times against simulated travel times to Jones Beach, there was fairly close agreement between observed and modeled values for the yearling Chinook salmon, especially in the negative rheotaxis and biased correlated random walk. Although the sample size for subyearling Chinook salmon in the pair trawl was small, there was also fairly close agreement between observed values and simulated values for the passive, random walk, and kinesis behaviors. In addition, the simulated travel times were within range of observed travel times described from the JSATS data, and the preferred migration pathways from simulations (i.e., greater occupation of navigation channel and WA 22) were also seen in the observations. Although direct comparisons with observed data were not possible in this application, the proximity of simulated travel times against observed travel times is a promising result and suggests that an IBM can be an effective tool for exploring migratory behavior of juvenile Chinook salmon in an estuarine environment.

Simulated growth rates in the IBM for subyearling Chinook salmon were within the range of growth rates reported from field observations, while those for yearling Chinook salmon were typically less than observed rates. Rich (1920) estimated growth rates of 0.44 mm d^{-1} from rkm 261 to the river mouth, while other studies have identified growth rates of 0.25 and 0.31 mm d^{-1} (McCabe et al., 1986; Roegner et al., 2012). Campbell (2010) studied otolith-derived growth estimates and determined mean daily growth rates of 0.41 mm d^{-1} for juvenile salmon in saline portions of the estuary. McNatt et al. (2016) documented mean growth rates of 0.49–0.58 mm d^{-1} for juveniles residing in wetlands, with length increases by as much as 10–20 mm for juveniles remaining in wetland areas longer than 15 days. Additional growth rates estimated from otolith analysis were on average 0.5 mm d^{-1} (Bottom et al., 2008). While it may be challenging to validate growth rates from the IBM, the growth rates were within the range of observed values, which lends support to the IBM being an effective tool for exploring how the estuary supports growth of juvenile Chinook salmon during their migration.

4.1. Limitations

IBMs have become an increasingly popular approach for simulating animal behavior and for exploring ecological questions. They offer a means by which we can test hypotheses and investigate how

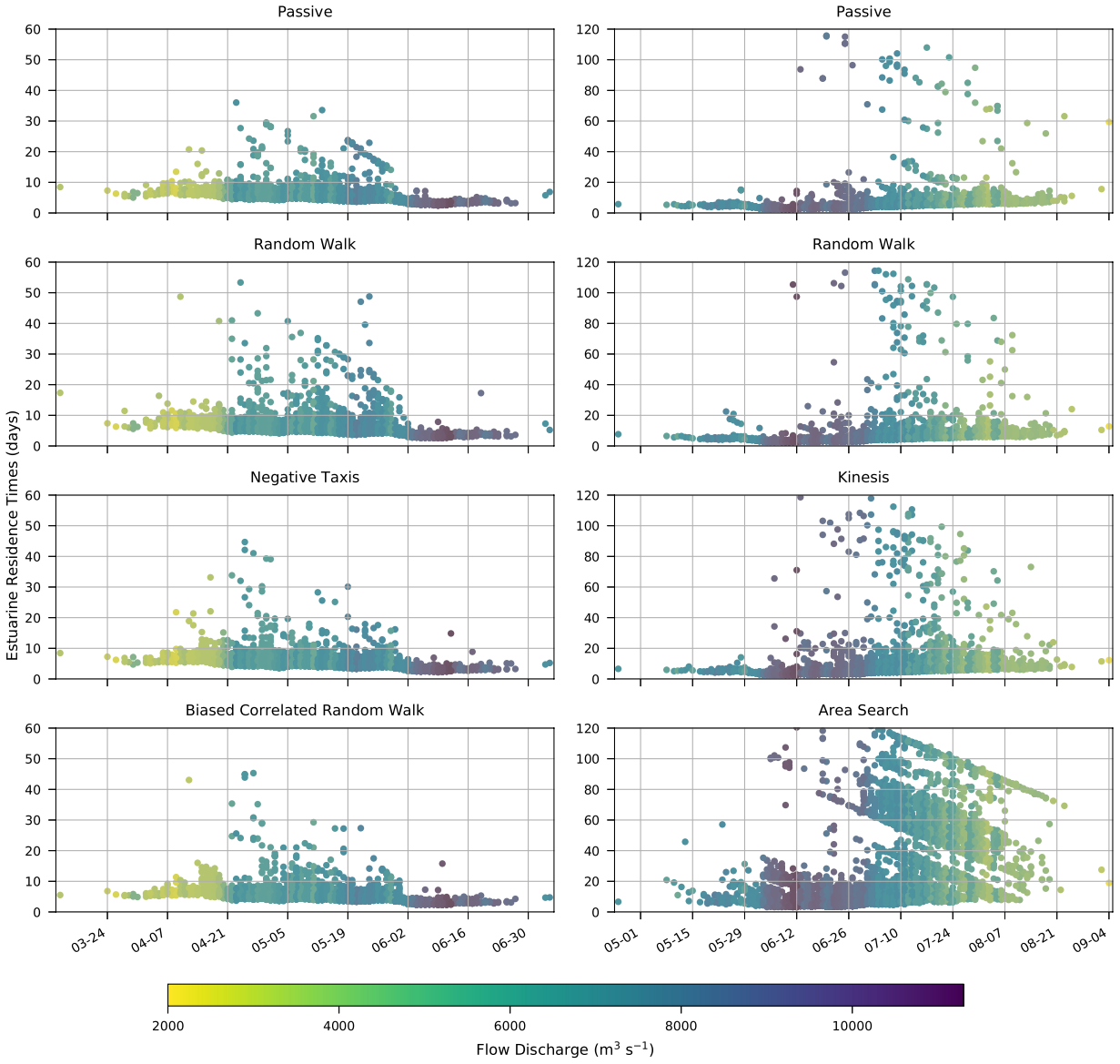

Fig. 9. Estuarine residence times (days) for simulated yearling Chinook salmon behaviors (*left*) and simulated subyearling Chinook salmon behaviors (*right*). Dates correspond with the date when fish were released at Bonneville Dam. Points are colored by the corresponding daily mean discharge on the day of release. (For interpretation of the references to color in this figure legend, the reader is referred to the web version of this article.)

environmental processes and individual behavior influence population-level dynamics. Despite advances in modeling techniques and computing power, IBMs continue to be limited. Since modeling relies on assumptions and simplification of behaviors, IBMs should not be expected to exactly mimic nature; however, they can be effective in answering questions that might be difficult to investigate using observations or Eulerian modeling techniques. This paper highlights the functionality of an IBM to investigate estuarine migration patterns of juvenile Chinook salmon, but it is important to note the limitations of our model and IBMs in general.

As juvenile Chinook salmon migrate from freshwater to brackish and increasingly marine waters, their behavior changes in response to ambient conditions. While the IBM effectively approximates movement, it is not a realistic representation of actual swimming behaviors through an evolving environment. The IBM is certainly an improvement from Eulerian-based methods that quantify salmon habitat for juvenile Chinook salmon, but there are still limits on its utility. Furthermore, juvenile Chinook salmon likely employ multiple strategies as they migrate through the system and rely on multiple cues simultaneously when making movement decisions. Their needs change over time, and they switch modes multiple times during their migration, from focusing on downstream movement to feeding and predator avoidance. In addition, there are larger-scale processes that influence their behavior, as well as their genetically-driven urge to migrate to the ocean. These environmental and behavioral drivers are constantly at play in different degrees. Since models are designed to simplify behavior to help us understand some of these dynamics, they will never accurately capture all of the more complex processes at play.

While including the bioenergetics model was a necessary component, especially as it influenced the swim speeds, there were limitations in how it was implemented. All of the standard equations used in the model worked well; however, the way in which prey energy density was approximated was overly simple. A constant prey energy density was used, and the *P*-value, which controls the amount of energy was based on proximity to wetland habitat. These methods of oversimplifying the bioenergetics model were somewhat necessary, as high-resolution data on salmon prey in the Columbia River estuary are limited. However, this oversimplification likely influenced results for individual growth

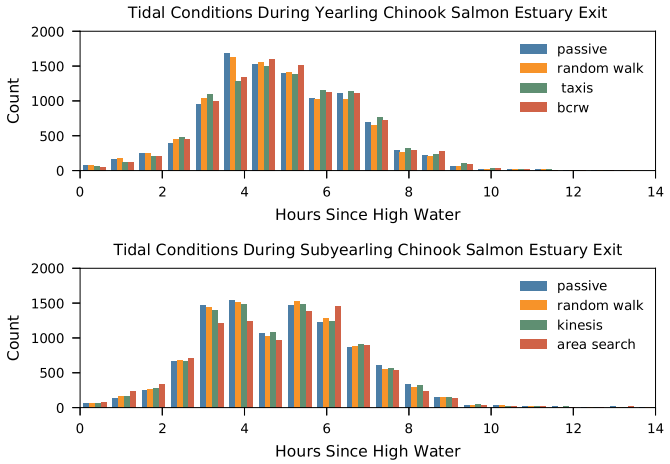

Fig. 10. Hours since high water at time of estuary exit for simulated yearling Chinook salmon (*top*) and simulated subyearling Chinook salmon (*bottom*). (For interpretation of the references to color in this figure legend, the reader is referred to the web version of this article.)

and may explain why yearling Chinook salmon growth showed such little variation and why the restricted-area search behavior led to such high growth rates.

Although simulated behaviors produced results that were within the range of observed travel times, model results should be interpreted with caution because predator avoidance was not considered as a behavioral response, and the cumulative effects of predation on migration patterns were not represented. Predation and mortality were not included in this version of the model due to the lack of high-resolution spatial and temporal observations on these top-down drivers. In addition, not enough is known about how juvenile Chinook salmon swimming behavior is influenced by predator avoidance, particularly in a system where flow velocities are so high. Even though information may be lacking, we acknowledge that predator avoidance could play a role in residence times and preferred migration pathways.

The hydrodynamic model used as the virtual environment for the IBM had some limitations, including the lack of freshwater flows imposed in the model that limited circulation in the smaller tributaries in the lateral bays. This led to the accumulation of passive particles or simulated fish in the shallowest upstream reaches of these tributaries. Kärnä and Baptista (2016b) mention that hydrodynamic model results in the lateral bays may not be reliable due to the lack of freshwater input and because of issues with the wetting-drying method, which is consistent with issues encountered in this work. In addition, most of the model skill validation for the circulation model focused on the main channels or deeper locations in the lateral bays. Thus, it is difficult to assess the skill of the circulation model in shallow regions. Lastly, the resolution of the bathymetry and size of the grid in shallow regions was limited, which affected migration pathways in shallow regions.

With regards to model-data comparisons, the pair-trawl and JSATS data were very valuable; however, the fish targeted in these studies were often not representative of the full diversity of sizes and life histories present in the estuary. Instead, they primarily targeted larger juveniles that remained in the main channels. In general, acoustic telemetry studies are rare in shallow habitats; however, there are some exceptions (Johnson et al., 2015; McNatt et al., 2016). Data describing travel times are likely inappropriate to apply to smaller subyearling Chinook salmon as they have longer residence times and are less likely to be tagged (see Bottom et al. 2005). Similarly, many of these tagging studies target fish from hatcheries and thus are not necessarily representative of behaviors associated with wild-type Chinook salmon.

5. Conclusions

An IBM was developed to explore estuarine migration pathways, residence times, and growth of juvenile Chinook salmon migrating through the Columbia River estuary. Multiple behaviors were implemented, ranging from random behaviors to more sophisticated behaviors that either optimized efficient migration through the system or opportunities for growth. Simulated behaviors for juvenile yearling

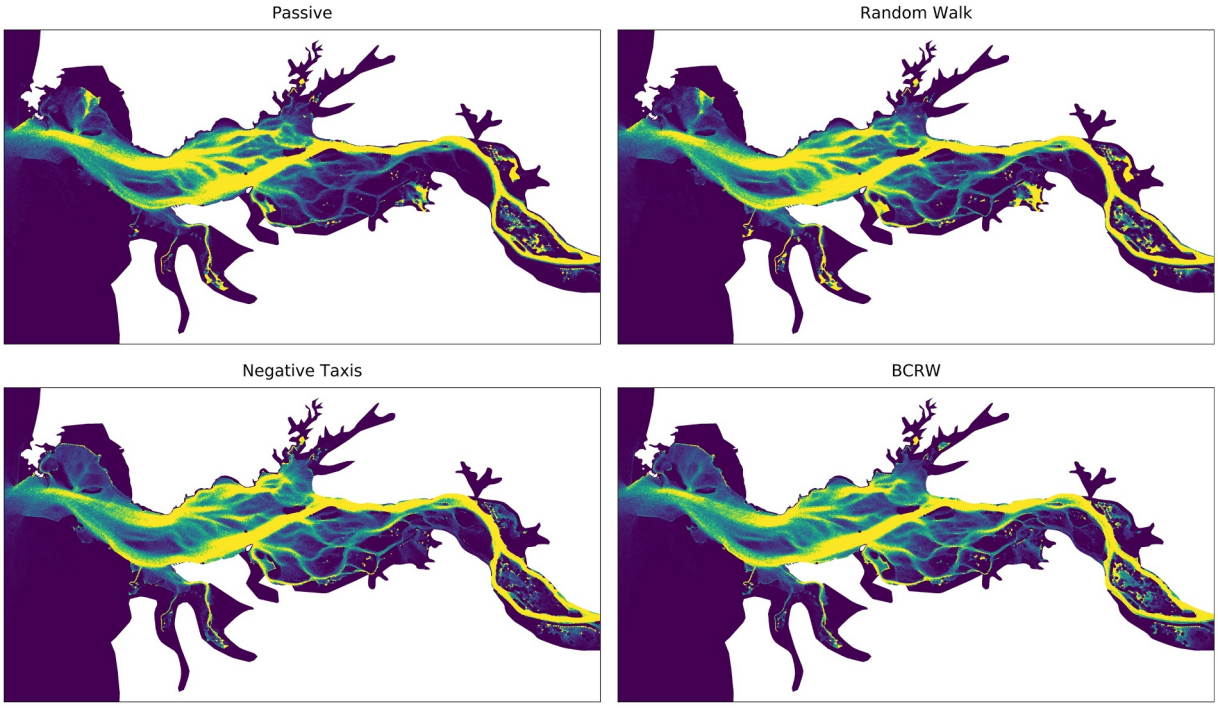

Fig. 11. Simulated migration pathways for yearling Chinook salmon, showing the number of times an element is occupied over time normalized by the element area for passive drift, random walk, negative rheotaxis, and biased correlated random walk behaviors. Yellow regions highlight common pathways. (For interpretation of the references to color in this figure legend, the reader is referred to the web version of this article.)

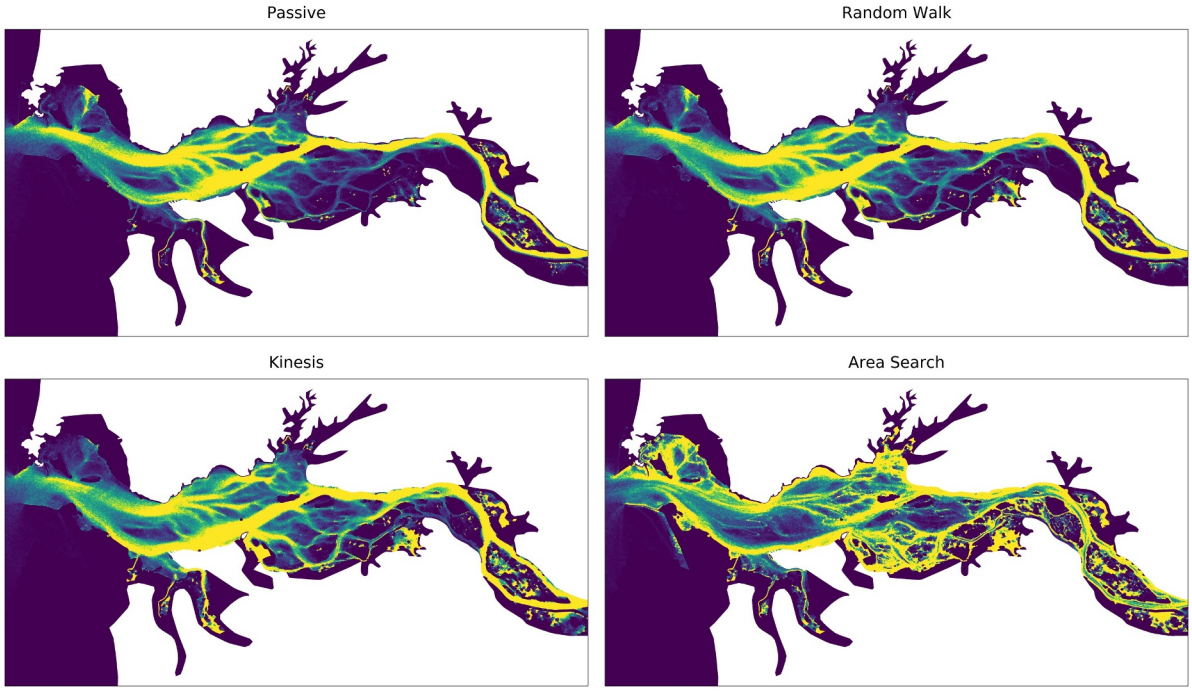

Fig. 12. Simulated migration pathways for subyearling Chinook salmon, showing the number of times an element is occupied over time normalized by the element area for passive drift, random walk, kinesis, and restricted-area search behaviors. Yellow regions highlight common migration pathways. (For interpretation of the references to color in this figure legend, the reader is referred to the web version of this article.)

Chinook salmon that optimized rapid migration outperformed the passive drift and random walk simulation due to reduced residence times. Similarly, the behaviors implemented for subyearling Chinook salmon that optimized increased growth resulted in higher growth rates when compared to the random walk behavior. In most simulations, residence times were on the order of days. River discharge had a strong influence on residence times, and during periods of high discharge, residence times were reduced.

While the model does have many limitations in its current implementation, it was effective for investigating how juvenile Chinook salmon respond to environmental forcing and behavioral controls. River discharge was a strong driver of residence times; however, active swimming and behavioral decisions made by individuals were also important in driving potential migratory pathways. The availability of PIT tag and JSATS tag data allowed for an in-depth model-data comparison. Consistent patterns in migration pathways and travel times between the simulated individuals and observed individuals suggest that this IBM could be used to inform management decisions by evaluating various scenarios.

Declaration of Competing Interest

The authors declare that they have no known competing financial interests or personal relationships that could have appeared to influence the work reported in this paper. The authors declare the following financial interests/personal relationships which may be considered as potential competing interests.

Acknowledgements

We would like to thank David Huff and Curtis Roegner for their guidance regarding juvenile salmon behavior and dynamics in the Columbia River estuary. We would also like to thank Matt Morris for his guidance regarding the pair-trawl data. In addition, we are grateful to those involved in the collection of JSATS data, including George McMichael, Ryan Harnish, and Gary Johnson. Special thanks also go to the Baptista group, including Paul Turner, Charles Seaton, Tuomas Kärnä, Jesse Lopez, and Mojgan Rostaminia. We would like to acknowledge the Columbia Basin PIT Tag Information System (PTAGIS), the Fish Passage Center's Smolt Monitoring Program, and Columbia Basin Research out of the School of Aquatic and Fishery Sciences at the University of Washington. This research was partially funded through the project “Sustaining NANOOS, the Pacific Northwest component of the U.S. Integrated Ocean Observing Systems”, Award NA16NOS0120019 of the National Oceanic and Atmospheric Administration. No NOAA personnel with influence on the funding was involved in the study design, collection of data, or writing of this paper.

References

Bailey, J.D., Wallis, J., Codling, E.A., 2018. Navigational efficiency in a biased and correlated random walk model of individual animal movement. Ecology 99, 217–223.
Baptista, A.M., Seaton, C., Wilkin, M.P., Riseman, S.F., Needoba, J.A., Maier, D., Turner, P.J., Kärnä, T., Lopez, J.E., Herfort, L., Megler, V.M., McNeil, C., Crump, B.C., Peterson, T.D., Spitz, Y.H., Simon, H.M., 2015. Infrastructure for collaborative science and societal applications in the Columbia River estuary. Front. Earth Sci. 9, 659–682.
Barron, C.N., Kara, A.B., Martin, P.J., Rhodes, R.C., Smedstad, L.F., 2006. Formulation, implementation and examination of vertical coordinate choices in the Global Navy Coastal Ocean Model (NCOM). Ocean Modell. 11, 347–375.
Benhamou, S., Bovet, P., 1992. Distinguishing between elementary orientation mechanisms by means of path analysis. Anim. Behav. 43, 371–377.
Booker, D.J., Wells, N.C., Smith, I.P., 2008. Modelling the trajectories of migrating Atlantic salmon (Salmo salar). Can. J. Fisher. Aquat. Sci. 65, 352–361.
Bottom, D.L., Anderson, G., Baptista, A., Burke, J., Burla, M., Bhuthimethee, M., Campbell, L., Casillas, E., Hinton, S., Jacobsen, K., Jay, D., McNatt, R., Moran, P., Roegner, G.C., Simenstad, C.A., Stamatiou, V., Teel, D., Zamon, J.E., 2008. Salmon Life Histories, Habitat, and Food Webs in the Columbia River Estuary: An Overview of Research Results, 2002-2006. pp. 52 National Oceanic and Atmospheric Administration, National Marine Fisheries Service, Northwest Fisheries Science Center, Fish Ecology and Conservation Biology Divisions, Seattle.
Bottom, D.L., Simenstad, C.A., Burke, J., Baptista, A.M., Jay, D.A., Jones, K.K., Casillas, E., 2005. Salmon at river's end: the role of the estuary in the decline and recovery of Columbia River salmon. In: Schiewe, M.H. (Ed.), NOAA Technical Memorandum NMFS-NWFSC-68.
Brosnan, I., 2014. Death of a Salmon: An Investigation of the Processes Affecting Survival and Migration of Juvenile Yearling Chinook Salmon (Oncorhynchus Tshawytscha) in the Lower Columbia River and Ocean Plume. Cornell University, Ithaca, New York.
Burke, B.J., Anderson, J.J., Baptista, A.M., 2014. Evidence for multiple navigational

sensory capabilities of Chinook salmon. Aquat. Biol. 20, 77–90.
Burke, B.J., Anderson, J.J., Miller, J.A., Tomaro, L., Teel, D.J., Banas, N.S., Baptista, A.M., 2016. Estimating behavior in a black box: how coastal oceanographic dynamics influence yearling Chinook salmon marine growth and migration behaviors. Environ. Biol. Fishes 99, 671–686.
Burla, M., 2009. The Columbia river estuary and plume: natural variability. Anthropogenic Change and Physical Habitat for Salmon. Oregon Health & Science University, Portland, Oregon.
Byron, C.J., Burke, B.J., 2014. Salmon ocean migration models suggest a variety of population-specific strategies. Rev. Fish Biol. Fish. 24, 737–756.
Campbell, L.A., 2010. Life Histories of Juvenile Chinook Salmon (Oncorhynchus tshawytscha) in the Columbia River Estuary as Inferred from Scale and Otolith Microchemistry. Oregon State University, Corvallis, Oregon.
Carter, J.A., McMichael, G.A., Welch, I.D., Harnish, R.A., Bellgraph, B.J., 2009. Seasonal Juvenile Salmonid Presence and Migratory Behavior in the Lower Columbia River. PNNL-18246. Pacific Northwest National Laboratory, Richland, Washington.
Codling, E.A., Hill, N.A., Pitchford, J.W., Simpson, S.D., 2004. Random walk models for the movement and recruitment of reef fish larvae. Marine Ecol. Progr. Ser. 279, 215–224.
Codling, E.A., Plank, M.J., Benhamou, S., 2008. Random walk models in biology. J. R. Soc. Interface 5, 813–834.
Cooke, S., Crossin, G., Hinch, S., 2011. Fish migrations | Pacific Salmon Migration: completing the cycle. Encycl. Fish Physiol. 3, 1945–1952.
Dawley, E.M., Ledgerwood, R.D., Blahm, T.H., Sims, C.W., Durkin, J.T., Kirn, R.A., Rankis, A.E., Monan, G.E., Ossiander, F.J., 1986. Migrational Characteristics, Biological Observations, and Relative Survival of Juvenile Salmonids Entering the Columbia River Estuary, 1966-1983. US Department of Energy, Bonneville Power Administration, Division of Fish & Wildlife.
Elliott, J.M., 1976. Energy losses in the waste products of brown trout (Salmo trutta L.). J. Anim. Ecol. 561–580.
Fiechter, J., Huff, D.D., Martin, B.T., Jackson, D.W., Edwards, C.A., Rose, K.A., Curchitser, E.N., Hedstrom, K.S., Lindley, S.T., Wells, B.K., 2015a. Environmental conditions impacting juvenile Chinook salmon growth off central California: an ecosystem model analysis. Geophys. Res. Lett. 42, 2910–2917.
Fiechter, J., Rose, K.A., Curchitser, E.N., Hedstrom, K.S., 2015b. The role of environmental controls in determining sardine and anchovy population cycles in the California Current: analysis of an end-to-end model. Progr. Oceanogr. 138, 381–398.
Fraenkel, G.S., Gunn, D.L., 1940. The Orientation of Animals: Kineses. Taxes and Compass Reactions, Oxford, pp. 352.
Giske, J., Huse, G., Fiksen, O., 1998. Modelling spatial dynamics of fish. Rev. Fish Biol. Fish. 8, 57–91.
Goodwin, R.A., Nestler, J.M., Anderson, J.J., Weber, L.J., Loucks, D.P., 2006. Forecasting 3-D fish movement behavior using a Eulerian–Lagrangian–agent method (ELAM). Ecol. Modell. 192, 197–223.
Grimm, V., Berger, U., Bastiansen, F., Eliassen, S., Ginot, V., Giske, J., Goss-Custard, J., Grand, T., Heinz, S.K., Huse, G., Huth, A., Jepsen, J.U., Jørgensen, C., Mooij, W.M., Müller, B., Pe'er, G., Piou, C., Railsback, S.F., Robbins, A.M., Robbins, M.M., Rossmanith, E., Rüger, N., Strand, E., Souissi, S., Stillman, R.A., Vabø, R., Visser, U., DeAngelis, D.L., 2006. A standard protocol for describing individual-based and agent-based models. Ecol. Modell. 198, 115–126.
Hamilton, K., Mysak, L.A., 1986. Possible Effects of the Sitka Eddy on Sockeye (Oncorhynchus nerka) and Pink Salmon (Oncorhynchus gorbuscha) Migration off Southeast Alaska. Can. J. Fish. Aquat. Sci. 43, 498–504.
Hanson, P.C., 1997. Fish Bioenergetics 3.0 For Windows. University of Wisconsin Sea Grant Institute, Madison, Wisconsin.
Harnish, R.A., Johnson, G.E., McMichael, G.A., Hughes, M.S., Ebberts, B.D., 2012. Effect of migration pathway on travel time and survival of acoustic-tagged juvenile salmonids in the Columbia River estuary. Trans. Am. Fish. Soc. 141, 507–519.
Healey, M.C., 1982. Juvenile Pacific salmon in estuaries: the life support system,. In: Kennedy,, V.S. (Ed.), Estuarine Comparisons. Academic Press, New York, pp. 315–341.
Healey, M.C., Thomson, K.A., Leblond, P.H., Huato, L., Hinch, S.G., Walters, C.J., 2000. Computer simulations of the effects of the Sitka eddy on the migration of sockeye salmon returning to British Columbia. Fish. Oceanogr. 9, 271–281.
Hinckley, S., Hermann, A.J., Megrey, B.A., 1996. Development of a spatially explicit, individual-based model of marine fish early life history. Mar. Ecol. Progr. Ser. 139, 47–68.
Humston, R., Ault, J.S., Lutcavage, M., Olson, D.B., 2000. Schooling and migration of large pelagic fishes relative to environmental cues. Fish. Oceanogr. 9, 136–146.
Humston, R., Olson, D.B., Ault, J.S., 2004. Behavioral assumptions in models of fish movement and their influence on population dynamics. Trans. Am. Fish. Soc. 133, 1304–1328.
Johnson, G.E., Ploskey, G.R., Sather, N.K., Teel, D.J., Fisk, A., 2015. Residence times of juvenile salmon and steelhead in off-channel tidal freshwater habitats, Columbia River, USA. Can. J. Fish. Aquat. Sci. 72, 684–696.
Kärnä, T., Baptista, A.M., 2016a. Evaluation of a long-term hindcast simulation for the Columbia River estuary. Ocean Modell. 99, 1–14.
Kärnä, T., Baptista, A.M., 2016b. Water Age in the Columbia River Estuary 183. Estuarine, Coastal and Shelf Science, pp. 249–259.
Kärnä, T., Baptista, A.M., Lopez, J.E., Turner, P.J., McNeil, C., Sanford, T.B., 2015. Numerical modeling of circulation in high-energy estuaries: a Columbia River Estuary benchmark. Ocean Modell. 88, 54–71.
Koehler, M.E., Fresh, K.L., Beauchamp, D.A., Cordell, J.R., Simenstad, C.A., Seiler, D.E., 2006. Diet and Bioenergetics of Lake-Rearing Juvenile Chinook Salmon in Lake Washington. Trans. Am. Fish. Soc. 135, 1580–1591.
Kukulka, T., Jay, D.A., 2003a. Impacts of Columbia River discharge on salmonid habitat: 1. A nonstationary fluvial tide model. J. Geophys. Res. 108.
Kukulka, T., Jay, D.A., 2003b. Impacts of Columbia River discharge on salmonid habitat: 2. Changes in shallow-water habitat. J. Geophys. Res. 108.
Ledgerwood, R.D., Ryan, B.A., Dawley, E.M., Nunnallee, E.P., Ferguson, J.W., 2004. A surface trawl to detect migrating juvenile salmonids tagged with passive integrated transponder tags. North Am. J. Fish. Manag. 24, 440–451.
McCabe, G.T., Emmett, R.L., Muir, W.D., Blahm, T.H., 1986. Utilization of the Columbia River estuary by subyearling Chinook Salmon. Northwest Sci. 60, 113–124.
McComas, R.L., McMichael, G.A., Vucelick, J.A., Gilbreath, L., Everett, J.P., Smith, S.G., Carlson, T.J., Matthews, G.M., Ferguson, J.W., 2008. A study to estimate salmonid survival through the Columbia River estuary using acoustic tags, 2006. National Marine Fisheries Service Report to the U.S. Army Corps of Engineers, Portland, Oregon.
McMichael, G.A., Eppard, M.B., Carlson, T.J., Carter, J.A., Ebberts, B.D., Brown, R.S., Weiland, M., Ploskey, G.R., Harnish, R.A., Deng, Z.D., 2010. The juvenile salmon acoustic telemetry system: a new tool. Fisheries 35, 9–22.
McNatt, R., Hinton, S., 2017. Evidence for Direct use of Tidal Wetlands by Interior Stocks of Juvenile Salmon, Anadromous Fish Evaluation Program, Annual Meeting, Richland, Washington.
McNatt, R.A., Bottom, D.L., Hinton, S.A., 2016. Residency and movement of juvenile Chinook salmon at multiple spatial scales in a tidal marsh of the Columbia River estuary. Trans. Am. Fish. Soc. 145, 774–785.
Miller, T.J., 2007. Contribution of individual-based coupled physical-biological models to understanding recruitment in marine fish populations. Mar. Ecol. Progr. Ser. 347, 127–138.
Mork, K.A., Gilbey, J., Hansen, L.P., Jensen, A.J., Jacobsen, J.A., Holm, M., Holst, J.C., Maoiléidigh, Ó, N., Vikebø, F., McGinnity, P., Melle, W., Thomas, K., Verspoor, E., Wennevik, 2012. Modelling the migration of post-smolt Atlantic salmon (Salmo salar) in the Northeast Atlantic. ICES J. Marine Sci. 69, 1616–1624.
Myers, E.P., Baptista, A.M., 2001. Inversion for tides in the Eastern North Pacific Ocean. Adv. Water Resour. 24, 505–519.
Myers, J.M., Kope, R.G., Bryant, G.J., Teel, D., Lierheimer, L.J., Wainwright, T.C., Grant, W.S., Waknitz, F.W., Neely, K., Lindley, S.T., 1998. Status Review of Chinook Salmon from Washington, Idaho, Oregon, and California 35. NOAA Technical Memorandum NMFS-NWFSC, pp. 443.
Okunishi, T., Ito, S.-I., Ambe, D., Takasuka, A., Kameda, T., Tadokoro, K., Setou, T., Komatsu, K., Kawabata, A., Kubota, H., Ichikawa, T., Sugisaki, H., Hashioka, T., Yamanaka, Y., Yoshie, N., Watanabe, T., 2012. A modeling approach to evaluate growth and movement for recruitment success of Japanese sardine (Sardinops melanostictus) in the western Pacific. Fish. Oceanogr. 21, 44–57.
Plumb, J.M., Moffitt, C.M., 2015. Re-estimating temperature-dependent consumption parameters in bioenergetics models for juvenile Chinook salmon. Trans. Am. Fish. Soc. 144, 323–330.
Politikos, D.V., Huret, M., Petitgas, P., 2015. A coupled movement and bioenergetics model to explore the spawning migration of anchovy in the Bay of Biscay. Ecol. Modell. 313, 212–222.
Prentice, E.F., Flagg, T.A., McCutcheon, C.S., Brastow, D.F., 1990. PIT-tag monitoring systems for hydroelectric dams and fish hatcheries. Am. Fish. Soc. Symp. 7, 323–334.
Quinn, T.P., 2005. The Behavior and Ecology of Pacific Salmon and Trout. University of Washington Press, Seattle, WA.
Railsback, S.F., Lamberson, R.H., Harvey, B.C., Duffy, W.E., 1999. Movement rules for individual-based models of stream fish. Ecol. Modell. 123, 73–89.
Rich, W.H., 1920. Early history and seaward migration of Chinook salmon in the Columbia and Sacramento rivers. Fish. Bull. 37, 1–74.
Roegner, G.C., McNatt, R., Teel, D.J., Bottom, D.L., 2012. Distribution, size, and origin of juvenile Chinook salmon in shallow-water habitats of the lower Columbia River and estuary, 2002–2007. Mar. Coast. Fish. 4, 450–472.
Rogers, E., DiMego, G., Black, T., Ek, M., Ferrier, B., Gayno, G., Janjic, Z., Lin, Y., Pyle, M., Wong, V., 2009. The NCEP North American mesoscale modeling system: Recent changes and future plans. In: Preprints, 23rd Conference on Weather Analysis and Forecasting/19th Conference on Numerical Weather Prediction.
Rose, K.A., Fiechter, J., Curchitser, E.N., Hedstrom, K., Bernal, M., Creekmore, S., Haynie, A., Ito, S.i., Lluch-Cota, S., Megrey, B.A., Edwards, C.A., Checkley, D., Koslow, T., McClatchie, S., Werner, F., MacCall, A., Agostini, V., 2015. Demonstration of a fully-coupled end-to-end model for small pelagic fish using sardine and anchovy in the California Current. Progr. Oceanogr. 138, 348–380.
Rostaminia, M., 2017. Change in Variability in the Columbia River Estuary: A Habitat Perspective. Oregon Health & Science University, Portland, Oregon.
Royce, W.F., Smith, L.S., Hartt, A.C., 1968. Models of oceanic migrations of Pacific salmon and comments on guidance mechanisms. Fish. Bull. 66, 441–462.
Sanborn Map Company, 2011. High resolution land cover. High Resolution Land Cover, Lower Columbia River Estuary. OR & WA, United States, 2007-2010. Sanborn Map Company, Portland, OR.
Simenstad, C.A., Burke, J.L., O'Connor, J.E., Cannon, C., Heatwole, D.W., Ramirez, M.F., Waite, I.R., Counihan, T.D., Jones, K.L., 2011. Columbia River estuary ecosystem classification—concept and application. US Geol. Surv.
Simenstad, C.A., Fresh, K.L., Salo, E.O., 1982. The role of Puget Sound and Washington coastal estuaries in the life history of Pacific salmon: an unappreciated function. Estuarine Comparisons. 14. Academic Press, New York, pp. 343–364.
Song, Y., Haidvogel, D., 1994. A semi-implicit ocean circulation model using a generalized topography-following coordinate system. J. Comput. Phys. 115, 228–244.
Stewart, D.J., Ibarra, M., 1991. Predation and production by salmonine fishes in Lake Michigan, 1978–88. Can. J. Fish. Aquat. Sci. 48, 909–922.
Stewart, D.J., Weininger, D., Rottiers, D.V., Edsall, T.A., 1983. An energetics model for lake trout, Salvelinus namaycush: application to the Lake Michigan population. Can. J. Fish. Aquat. Sci. 40, 681–698.

Thornton, K.W., Lessem, A.S., 1978. A temperature algorithm for modifying biological rates. Trans. Am. Fish. Soc. 107, 284–287.
Thorpe, J.E., 1994. Salmonid fishes and the estuarine environment. Estuaries 17, 76–93.
Tyler, J.A., Rose, K.A., 1994. Individual variability and spatial heterogeneity in fish population models. Rev. Fish Biol. Fish. 4, 91–123.
Ware, D., 1978. Bioenergetics of pelagic fish: theoretical change in swimming speed and ration with body size. J. Fisher. Board Can. 35, 220–228.
Watkins, K.S., Rose, K.A., 2013. Evaluating the performance of individual-based animal movement models in novel environments. Ecol. Modell. 250, 214–234.
Watkins, K.S., Rose, K.A., 2017. Simulating individual-based movement in dynamic environments. Ecol. Modell. 356, 59–72.
Weitkamp, L.A., Bentley, P.J., Litz, M.N.C., 2012. Seasonal and interannual variation in juvenile salmonids and associated fish assemblage in open waters of the lower Columbia river estuary. Fish. Bull. 110, 426–450.
Weitkamp, L.A., Goulette, G., Hawkes, J., O'Malley, M., Lipsky, C., 2014. Juvenile salmon in estuaries: comparisons between North American Atlantic and Pacific salmon populations. Rev. Fish Biol. Fish. 24, 713–736.
Willis, J., 2011. Modelling swimming aquatic animals in hydrodynamic models. Ecol. Modell. 222, 3869–3887.
Zhang, Y., Baptista, A.M., 2008. SELFE: a semi-implicit Eulerian–Lagrangian finite-element model for cross-scale ocean circulation. Ocean Modell. 21, 71–96.